J Bio Tribo Corros (2015) 1:28
DOI 10.1007/s40735-015-0024-x

REVIEW PAPER

A Review on TiO_2 Nanotubes: Influence of Anodization Parameters, Formation Mechanism, Properties, Corrosion Behavior, and Biomedical Applications

K. Indira[1,3] · U. Kamachi Mudali[2] · T. Nishimura[3] · N. Rajendran[1]

Received: 23 June 2015 / Revised: 26 July 2015 / Accepted: 1 August 2015 / Published online: 7 October 2015

Abstract In this article, influence of anodization parameters on the formation of tubes, tube dimensions, formation mechanism, properties of TiO_2 nanotubes (TNT), and their applications in biomedical field are reviewed. The fabrication of TNT of a different shape such as pore size, length, and wall thickness by varying anodization parameters including electrolytes, pH, voltage, electrolyte bath temperature, and current density is examined and discussed. The crystallographic nature of the nanotube obtained by various methods has also been discussed. Finally, the article concludes by examining the key properties including the corrosion aspect and various applications in biomedical field in depth.

Keywords TiO_2 nanotubes · Oxide dissolution · Amorphous · Corrosion · Biomedical applications

1 Introduction

Now-a-days, a wide range of materials are required to design and study modern devices, which are suitable for various possible commercial applications. Nanomaterials play an important role in recent technologies to reach high-performance devices. The performance of such devices is significantly determined by geometry, shape, and morphology of nanostructures [1]. Exponential growth in the literature addresses that the nanoscale began at 1990's [2]. Interest in the nanoscale has been driven by the commercial availability of nanoscale manipulation and characterization tools due to the following reasons: (1) expectation of new physical, chemical, and biological properties of nanostructures, (2) expectations that the nanostructure provides new building blocks for innovative new materials with novel properties, (3) miniaturization into the nanoscale by the semiconductor industry, and (4) recognition that the molecular machinery in a biological cell functions at the nanoscale [3]. Historical aspects of chemistry and biology such as colloids, protein engineering, and molecular virology have involved nanostructures but on a largely empirical basis. Finally, there is an expectation that a better understanding of the 1–100 nm size materials (nanoscale) leads to a seamless integration of theory and models across the size scales that encompass atomic–molecular nanostructure–microstructure behavior, and thereby enable the priori prediction and design of a material's properties [4].

In this concern, one-dimensional nanostructure-like nanotubes can exhibit large internal and external surfaces along with surface in their vertex and a surface in the interlayer regions [5]. Among the various nanostructured oxide materials, special attention has been directed to TiO_2 nanotubes (TNT) due to its enhanced properties, cost-effective construction, and higher surface-to-volume ratio [6]. The TNT with high-specific surface area, ion-exchangeable ability, and photocatalytic property has been considered for various potential applications as catalyst in pool boiling [7], photocatalysis [8–17], electro chromic device [18–21], hydrogen generation [22, 23], corrosion resistance [24], solar cells [25–28], sensors [29–36], storage device [37, 38], catalyst support [39], wastewater

✉ N. Rajendran
nrajendran@annauniv.edu

[1] Department of Chemistry, Anna University, Chennai 600 025, India

[2] Corrosion Science and Technology Group, Indira Gandhi Centre for Atomic Research, Kalpakkam 603 102, India

[3] Materials Recycling Design Group, Research Centre for Strategic Materials, National Institute for Materials Science, Tsukuba, Japan

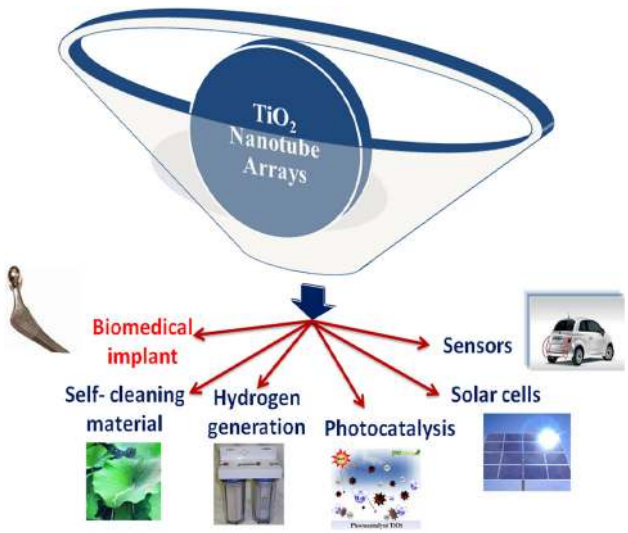

Fig. 1 Schematic illustration of applications of TNT

treatment [40], wettability [41, 42], and especially in the biomedical field [43–49]. Figure 1 shows the above-mentioned applications schematically. In addition to the aforementioned applications, now-a-days the TNT is used to remove the environmental pollutants [50] and as a volatile organic content sensor [51].

In the biomedical field, clinical applications with implants often fail because the implant surface do not support with new bone growth, which leads to its insufficient bonding to juxta posed bone, and thus the formation of fibrous tissue [52]. In order to overcome this, the surface of the implant should be modified. Calcium phosphate (HAp) grown TNT could be used as an implant material due to its outstanding biocompatibility and good osseo-integration. As far our knowledge, yet there are no reports available on the use of this kind of implants in human beings. However, some reports are available on the use of TNT as an implant in the animals. Wilmowsky et al. [53] investigated the effects of TNT on peri implant bone formation in vivo using Pig. Yet another report by Wang et al. [54] showed the effect of TNT on biological attachment mechanism of implants to bone in vivo by studying the gene expression and bone formation around the implant in pigs. Hence, the present review article focuses mainly on the various methods involved in the development of TNT, various parameters that affect the tube formation, tube forming mechanism, properties, and its application in biomedical field which is schematically illustrated in Fig. 2.

1.1 Various Methods for the Development of TNT

Numerous methods are available for the development of TNT, which includes anodization [55–65], sol–gel method [66–69], template method [70–72], hydrothermal method [38, 73–81], sonoelectrochemical [82–85], micro-wave irradiation [86, 87], and alkaline synthesis [88]. Hoyer [89] was first reported the synthesis of TiO_2-based nanotubes via template-assisted synthesis. Thereafter, electrochemical anodization and hydrothermal methods were succeeded in fabricating TNT [90].

Among all these methods, electrochemical anodization is widely used because of its controllable, reproducible results as well as single process, the feasibility to tune the size and shape of nanotubular arrays to the desired dimensions and meeting the demands of specific applications by means of controlled anodic oxidation of the metal substrate. Furthermore, it is a cost-effective method and the tubes prepared via this method have good adherent strength. In addition, the thickness and morphology of TiO_2 films can easily be controlled by the anodization parameters [91, 92]. Figure 3 shows the schematic illustration of anodization set up and the resultant nanotubular structure.

1.2 Nanotube Arrays on Ti Alloys

Nanotubes can also be fabricated using Ti alloys as substrate materials. However, most of the Ti alloys used in engineering/biomedical applications show a dual phase that is $\alpha + \beta$ microstructure. The α phase, which has a hexagonal close packing (hcp) structure, is enriched with hcp stabilizing elements such as Al, O, N etc., whereas β-phase with body-centered cubic (bcc) structure is enriched with the β-stabilizing elements such as V, Nb, Mo, Ta, etc. The formation of uniform nanotubular oxide layer on Ti alloys having dual phase microstructure cannot be achieved which is due to the difference in chemistries of these phases, as one phase could get etched preferently by the electrolyte. It was envisaged that the differences in chemistries and dimensions of nanotube on Ti alloys could render interesting electronic and physical properties that can be modulated for a wide variety of applications [29]. The mainly used Ti alloys for the formation of nanotubes are Ti–Nb [93], Ti–Ta [94], Ti–Al–Zr [95], Ti–Zr [96], Ti–29Nb–13Ta–4.6Zr [97], Ti–Mn [83], Ti–6Al–4V [98], and Ti–6Al–7Nb [99].

1.3 Doping of TNT with Other Elements

Most recent research on TNT focuses on the doping or deposition of some metal ions such as Ta [100], Au [33, 68, 101], Ag [102–104], Ru [105], B [106], Fe [107], Cu [69], Pd [108], Pt [109, 110], Ni [111, 112], Cr [113], Nd [114], Sr [115, 116], Zr [117, 118]; and non-metals like C [20, 119–122], N [123, 124], and F and B [125]; and metal oxides like MnO_2 [126] had enhanced its applications in many fields. Most recently, Loget et al. [127] coated biomimetic polydopamine into TNT for the development of

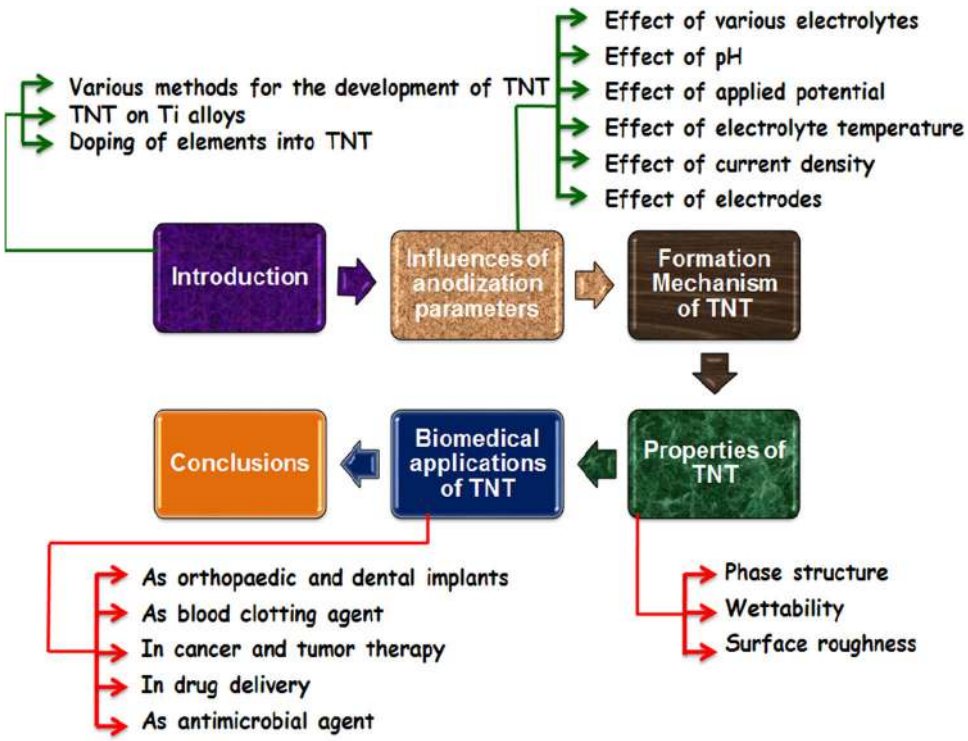

Fig. 2 Outline of the present review article

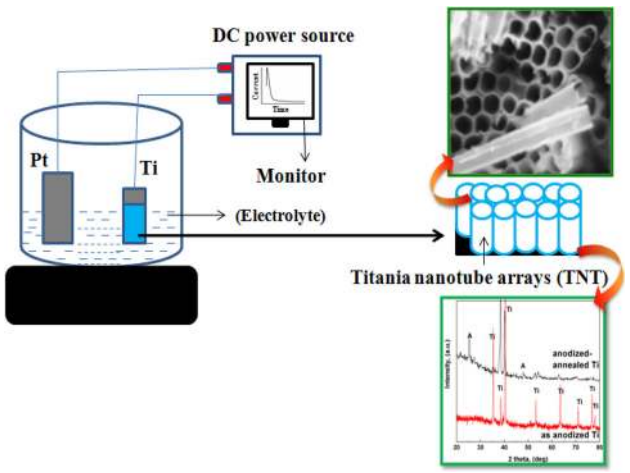

Fig. 3 Anodization set up and the structure of resultant TNT

biomedical devices. Similarly, graphene oxide coating has been done on TNT for biomedical applications [128]. The TNT can be used as a field emission electron source for generating X-ray radiation. It is not affected by exposure to O_2 and has a good electrical contact between TNT film and conductive Ti sheet [129].

In our earlier studies, we have incorporated Sr and Zr ions onto TNT for orthopedic implant applications [115, 117]. Figure 4 shows the micrograph of TNT after the incorporation of Sr and Zr ions. The tubular structure of TNT is retained with the small reduction in the diameter of tubes after the incorporation of Sr and Zr (20 and 15 nm reduction for Sr and Zr, respectively). We found that the Sr and Zr incorporated TNT has enhanced bioactivity and higher corrosion resistance than the TNT without Sr and Zr ions. Very recently, Chen et al. [130] developed TNT-Au@Pd hybrid nanostructures for the non-enzymatic sensing applications. The materials are highly sensitive, fast response, and having excellent electrocatalytic activity. Graphene oxide nanosheets have been deposited on TNT by electrophoretic deposition for application as photo-anodes in high-efficiency dye-sensitized solar cells [131].

2 Influences of Anodization Parameters

Great attention has been drawn on the formation of nanotubes which were known to be affected by the electrolyte concentration, electrolyte pH, anodization voltage, time, and temperature [23]. Therefore, the following section provides the comprehensive review on the influences of aforementioned parameters on the formation of TNT.

2.1 Effect of Electrolytes

The nature of electrolyte used for the development of TNT strongly influences the formation of the graded structure. It was well recognized that under the same conditions, different electrolytes may produce different electric field

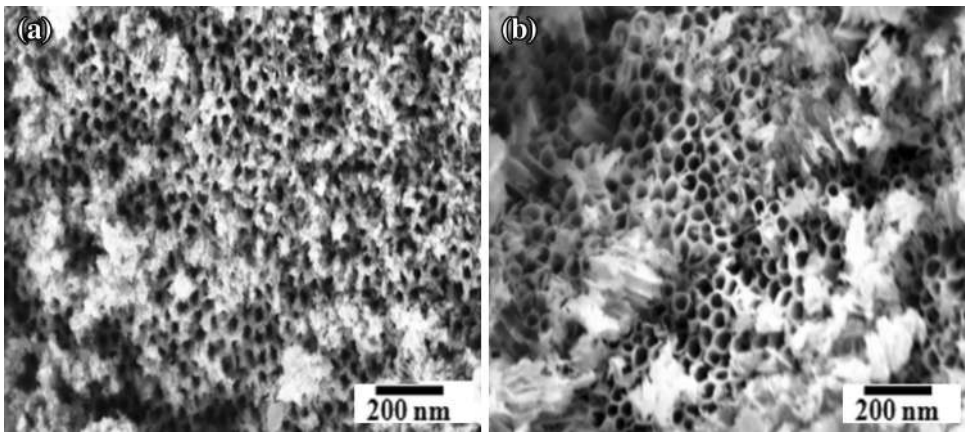

Fig. 4 SEM images of TNT after the incorporation of **a** Sr and **b** Zr ions

intensities. It was also well known that in the initial stage of anodization, the higher electric field intensity can induce bigger breakdown sites which finally result in wider diameter of TNT. Additionally, the chemical dissolution rate of oxide layer is also discrepant in different electrolytes. In other words, one can obtain different titanium oxide structures such as a flat compact oxide, a disordered porous layer, a highly self-organized porous layer, and/or finally a highly self-organized nanotubular layer by controlling the electrochemical anodization parameters of Ti [132].

The TNT can be synthesized by anodization using various fluoride-containing electrolytes like NH_4F/CH_3COOH, H_2SO_4/HF, Na_2HPO_4/NaF, etc. The nanotube diameter is remarkably affected by the electrolytes used [63]. Generally, two different types of electrolytes such as organic (or neutral) and aqueous electrolytes have been used for the synthesis of TNT. When the anodization takes place in an acidic condition of pH, in other words, high water content is called aqueous electrolytes. An organic (or neutral) electrolyte has a small amount of oxygen/water content in comparison to an aqueous electrolyte.

In the organic electrolyte like $(NH_4)H_2PO_4/NH_4F$ [57] and $(NH_4)_2SO_4/NH_4F$ [133], longer nanotube length and better self-organized TNT layers were obtained. These self-organized porous structures have large potential and commercial applications in view of several interesting properties. Yang et al. [134] reported that in order to obtain long TNT, fluoride-containing electrolytes should be used in place of HF-containing buffer electrolytes species of highly viscous (organic) electrolytes. Neutral and viscous electrolytes allow better control in the anodic conditions and creating two different environments along the tube, one inert at the top of it and other chemically reactive at the bottom. Thus, the inhibition of the oxide dissolution at the top side of the nanotube allows the formation of longer TNT [135]. Much higher current densities are observed in the aqueous electrolytes than in the organic electrolyte [136], which is attributed to higher diffusibility and concentration of ions in aqueous electrolytes. However, smooth curves were obtained at all voltages in the glycerol (organic) electrolytes, whereas current fluctuations were observed in aqueous electrolyte which is due to the high rate of chemical dissolution and the oxidation of Ti [137].

We have reported in our earlier study that, depending on the electrolytes, the pore diameter alters and also its concentration effected the porous structures formation [138]. Figures 5 and 6 show the SEM micrographs of the anodized samples at 0.1, 0.15, and 0.2 M HF concentration in aqueous and organic electrolyte. Under optimized electrolyte conditions, titania nanopore is obtained with the average pore diameter of 64 nm and 84 nm for aqueous (mixture of 0.13 M H_2SO_4 and HF) and (mixture of 0.13 M glycerol and HF) organic electrolytes, respectively, at 0.10 M HF concentration. Atomic force microscopic investigation shows that the porous layer forms under a competition of titania formation and oxide dissolution up to a limiting thickness of $\sim$75 and 100 nm, respectively, for aqueous and organic electrolytes. The length of the oxide layer was found to be 3 and 3.5 μm for aqueous and organic electrolyte, respectively. The porous structure was observed at 0.15 M HF concentration, below and above which no pores were formed.

Furthermore, it is also evident that the layer in the acidic electrolytes is relatively thin compared to neutral electrolyte. This difference must be ascribed to pH dependence of the oxide dissolution rate [139]. Aqueous electrolytes like H_3PO_4/HF [140], HF/NH_4F [141] etc., provide well-ordered TNT. According to Chen et al. [142], smaller TNT was obtained using CH_3COOH/NH_4F electrolytes and can be replaceable by the environment benign electrolytes such as HCl/NH_4F electrolytes. Highly ordered TNT was obtained in malonic acid solution [143]. Similarly, Tian et al. [144] reported that TNT formed in H_2SO_4 electrolyte exhibited a variation in the tube length, which depends on its concentration; the inner diameter of nanotubes

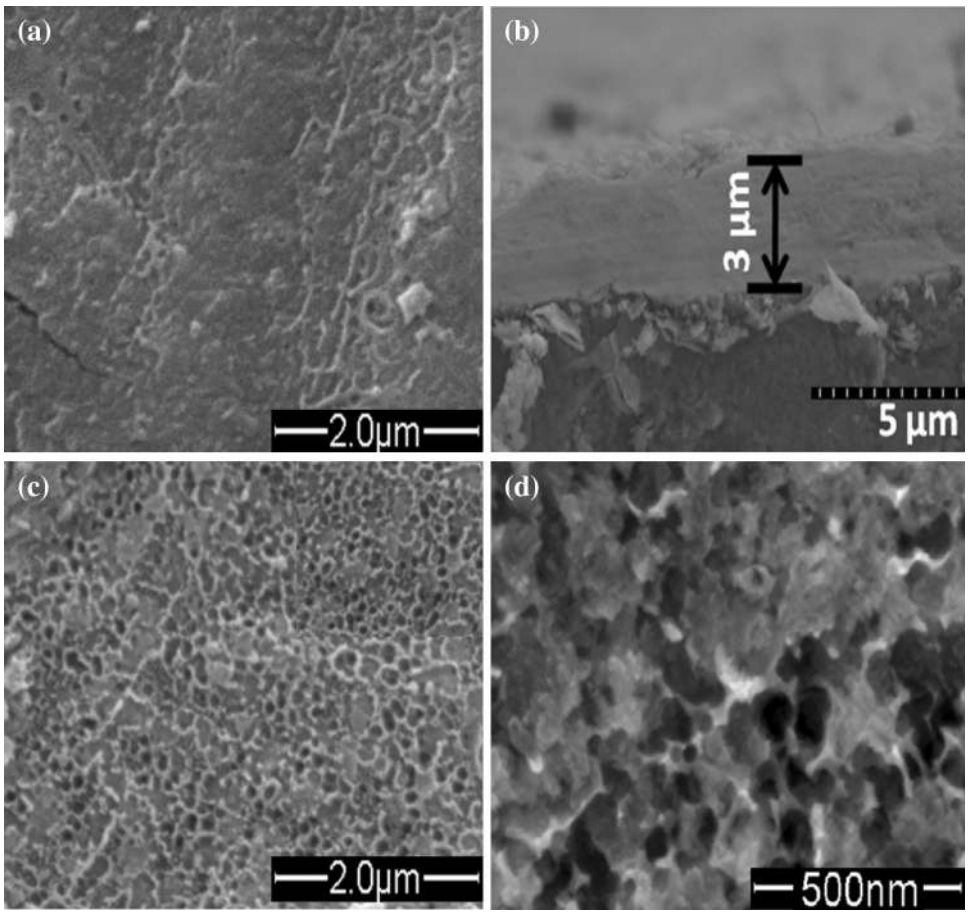

Fig. 5 SEM images of the anodized Ti at 40 V in 0.13 M H_2SO_4 with different HF concentrations: **a** 0.1 M HF, **b** cross-sectional view **c** 0.15 M HF and **d** 0.2 M HF

decreases with H_2SO_4 concentration from 120 to 100 nm in 0.24 mol/l M H_2SO_4 and 1.75 mol/l M H_2SO_4, respectively. The difference in concentration leads to significant variations of the structure of Ti. The sponge-like feature was observed at 0.10 wt% NH_4F, and at 0.50 wt% NH_4F, nanotubular structure is clearly visible. The NH_4F concentration is beneficial to the growth of TNT to a certain extend [145]. In addition, TNTs were developed in fluoride-free electrolytes too. Hahn et al. [146] had successfully developed high-aspect ratio TNTs using fluoride-free approach i.e., the anodization in perchlorate and chloride-containing electrolytes. The ultrahigh-aspect ratio TNT was fabricated by anodization in electrolytes containing oxalic, formic, or sulfuric acid and chlorine ions. Chlorine-based (fluoride-free) electrolytes have an advantage over fluoride containing one. In the fluoride-free electrolyte, long TNT can be grown in a very short time (growth rate is >1000 times faster than in fluorine media; e.g., 10 min in chlorine-based electrolytes compared to ~17 h in fluorine-based electrolytes) [147]. Nguyen et al. [77] were developed TNT in fluoride-free electrolytes with bromide anions in various solvents, including ethylene glycol, glycerol, and water–ethylene glycol and water–glycerol mixtures. They found that tubes grown in Br-based electrolyte do not have the self-organized structure of those seen in fluoride solutions, the growth rates are much faster, achieving tens of microns in length in 60s.

Further, reusing the electrolyte solution, which was electrolyzed by previous anodization run, resulted in a better nanotubular morphology than the morphology observed using fresh electrolyte solution [148]. Compared to that observed for the freshly prepared electrolyte, reusing the electrolyte as the second time was found to give the larger pore diameter and the smaller wall thickness, which is attributed to the pronounced effect of more chemical etching or more oxide dissolution influenced by the improved electrolyte conductivity. Normally, after anodization, the field-assisted dissolution led to the dissolution of more titanium ions into the electrolyte; thus, it gives rise to the high electrolyte conductivity. This could in turn fasten the reaction processes in the second anodization and consequently influence the nanotube morphologies. Affected by the electrolyte properties, the increased conductivity of the used electrolyte is believed to play a major role in governing the nanotube formation, and thus determining the consequent film properties [149].

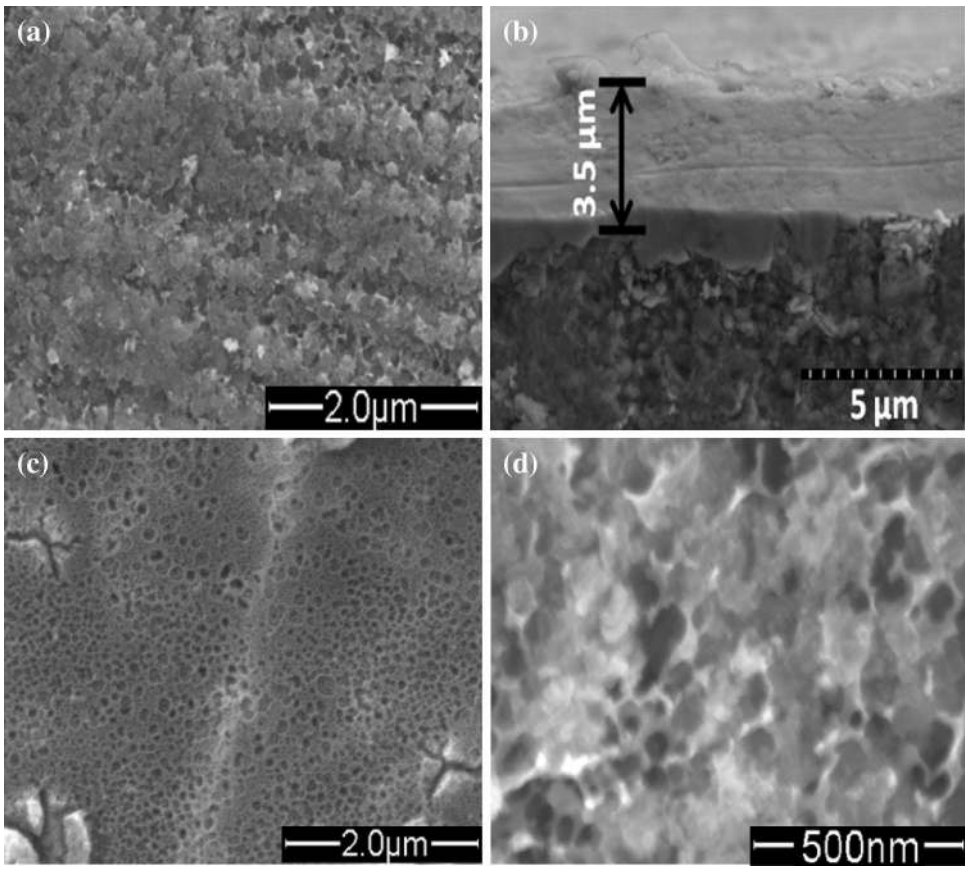

Fig. 6 SEM images of the anodized Ti at 40 V in 0.13 M glycerol with different HF concentrations: **a** 0.1 MHF, **b** cross-sectional view, **c** 0.15 M HF and **d** 0.2 M HF

2.2 Effect of Electrolyte pH

The pH of the electrolyte is the key to achieve growth of the high-aspect ratio nanotubes and it can affect the self-organization behavior of TNT. The difference in the pH leads to significant variations in the pore diameter. The differences in thickness are attributed to pH dependence of the oxide dissolution rate, i.e., dissolution rate at low pH is much greater than the higher pH [150]. Therefore, the pH alters the thickness and diameter of the pores. It has been reported that a mixture of 1 M Sodium hydrogen sulfate monohydrate and 0.1 M KF with 0.2 M Sodium citrate tribasic dehydrate electrolyte shows the variation in the nanotube length from 380 nm to 6 μm and tube diameters from 30 to 110 nm, which is due to the electrolyte pH and anodization potential [151]. The pH value of the electrolyte changes during anodization because of several other reasons [152]. The formation of hydrolysis product at the working electrode leads to the decreases in pH; thus, the local acidification is established. Tailoring the local acidification could promote the TiO_2 dissolution, thereby providing more protective environment against the dissolution along the tube mouth, thus, longer tubes were obtained. Hydrogen evolution and OH^- species formation take place at the counter electrode [153, 154].

2.3 Effect of Applied Voltage

The applied voltage strongly influences the pore diameter, inter pore distance, and film thickness in a wide range [123]. Subsequently, the morphology of the layer is strongly affected by the applied voltage and anodization time. At low applied voltages, tubes with few hundreds of nanometer in length and a few tens of nanometer in diameter were formed. In the short-term anodization, the individual tubes are connected with each other via rings on the side walls of the tubes, whereas in the longer-term anodization, tubes were separated due to the dissolution of these rings [136].

The most regular porous structure is obtained at the applied voltage of 20 V. The films formed at potentials below 20 V exhibit a nanoporous but thinner structure. In this case, the layers do not thicken more, because the current is not sufficiently high. It has been reported that the films formed between 22 and 30 V have tubular but irregular porous structure. Above 30 V, large cracked areas of porous oxide film were formed at the interface film substrate with a diameter in the micrometer scale, which can be attributed to breakdown events at high potentials [155]. At low anodizing voltages, the morphology of the porous film is similar to that of porous alumina. As the

voltage was increased, the surface becomes particulate or nodular in nature. As the voltage was further increased, the particulate appearance is lost and discrete, hollow, cylindrical tube-like features was created. The structure of nanotube is lost at anodizing voltage greater than 40 V, and a sponge like randomly porous structure was formed [137].

The chemical dissolution of TiO_2 layer plays a crucial role in the TNT formation. As we already seen in the previous section, the chemical dissolution rate of TiO_2 is obviously a highly pH-dependent process [151, 156]. Since high acidic condition was established at the bottom of tubes due to the formation of hexafluoro titanium complex (detailed mechanism is given below in the following section), tubes would preferentially continue to grow down to the bottom of metal foil, resulting in tubular structures. Subsequently, high potential will impose more force on the dissolution of oxide by F-ions, the pore size of the TNT will be therefore larger and tube length longer at high anodizing potentials when organic electrolytes were employed [157]. Generally, the dissolution rate is high in the acidic electrolytes due to the higher pH (local acidification) at the bottom of tubes [156], if more potential is applied in addition to these results in too much dissolution rate, thus it led to permanent dissolution of oxide layer and no tube formation could be observed. Hence, it is preferential to apply lower voltages for the acidic electrolytes and higher voltages for the organic electrolytes.

2.4 Effect of Electrolyte Temperature

Self-organized nanotubes are formed in glycerol electrolyte at temperatures of 0, 20, and 40 °C. At temperatures higher than 40 °C, only unstable bundles of tubes can be formed on the Ti surface and no regular and mechanically stable nanotubular structure can be obtained [158]. Figure 7a–d presents the SEM micrographs of anodized Ti at 5, 10, 15, and 20 °C. Thick porous oxide layer was formed at 5 °C (Fig. 7a), porous structure with irregularly ordered pores rather than a typical ordered pores are visible at 10 °C (Fig. 7b) and a regular pores are formed at 15 °C (Fig. 7c), the diameter of the pores are found to be in the range of 45–50 nm. In addition, it is observed that two to three new smaller pores inside these existing pores are created. Further increase in temperature leads to a well-ordered pores with the diameter of 84 nm. From this result it is obvious that the pore formation increases with increasing the electrolyte temperature [159]. This may be the reason that the viscosity of the electrolyte was reduced in the higher temperature [160] leading to faster etching rate. When etching becomes fast, the oxide layer gets dissolved faster and form pores. At lower temperature, the mobility of fluoride ions was suppressed, which leads to slower etching rate [161]. Due to the slower etching rate of the oxide layer, no regular pores were formed at lower temperatures.

2.5 Effect of Current Density

Different current densities produce different pore sizes, which impact the electrochemical etching rate. As the current density increases, the electrochemical etching rate, power, and electric field intensity also increase. These effects appear to cause pit widening before the formation of channels, which form separate pores. As the current density of Ti foil increases further, pore size of TNT also increases. Consequently, different tube diameters could be produced by controlling the current density [133]. The current density measurement at constant voltage in fluoride-containing solutions reflects the progress of TNT layer formation. The current density in fluoride-containing electrolytes is higher than those in fluoride-free electrolytes, and increase with increasing the fluoride content in the range of 0–2 wt%. The formation of TNT is clearly affected by fluoride ion. A key factor which influences the electrochemistry of TNT formation is the fluoride ion concentration in the electrolyte [161]. Figure 8 shows the current–time transient at various electrolytes and voltages [115, 138]. The aqueous electrolyte showed higher current value than the organic electrolytes. The increase in the current density and the subsequent appearance of the broad current maximum reveal the local breakdown of an initially formed compact oxide layer and the starting of the nanotube structure development, respectively [162].

2.6 Effect of Anodization Time

The anodization time also influences greatly on the TNT formation mechanism. There has no TNT, if the anodization time is too short. According to Li et al. report [163], the minimum time needed for the formation of TNT is 15 min, with increase in time highly ordered TNT can be formed. Similarly, Regonini and Clemens [164] found that at the anodization time of 5 min, only nanoporous structure was formed, and only after 10–20 min, the nanotubular structure was visible clearly. A short and narrow TNT can be easily obtained in short growth time (i.e., 5-min anodization time) [165]. A report by So et al. [166] showed that highly ordered TNT with the thickness of 7 μm can be grown in 25 s using Lactic Acid as an additive to the electrolyte. They showed that Lactic Acid can effectively prevent localized dielectric breakdown of the anodic oxide at elevated anodization voltages; thus, it allows establishing a higher ion transport through the oxide film and, as a result, extremely fast tube growth rates without losing the tube's functional properties. By extending the anodization time, the length of TNT has been increased. If the

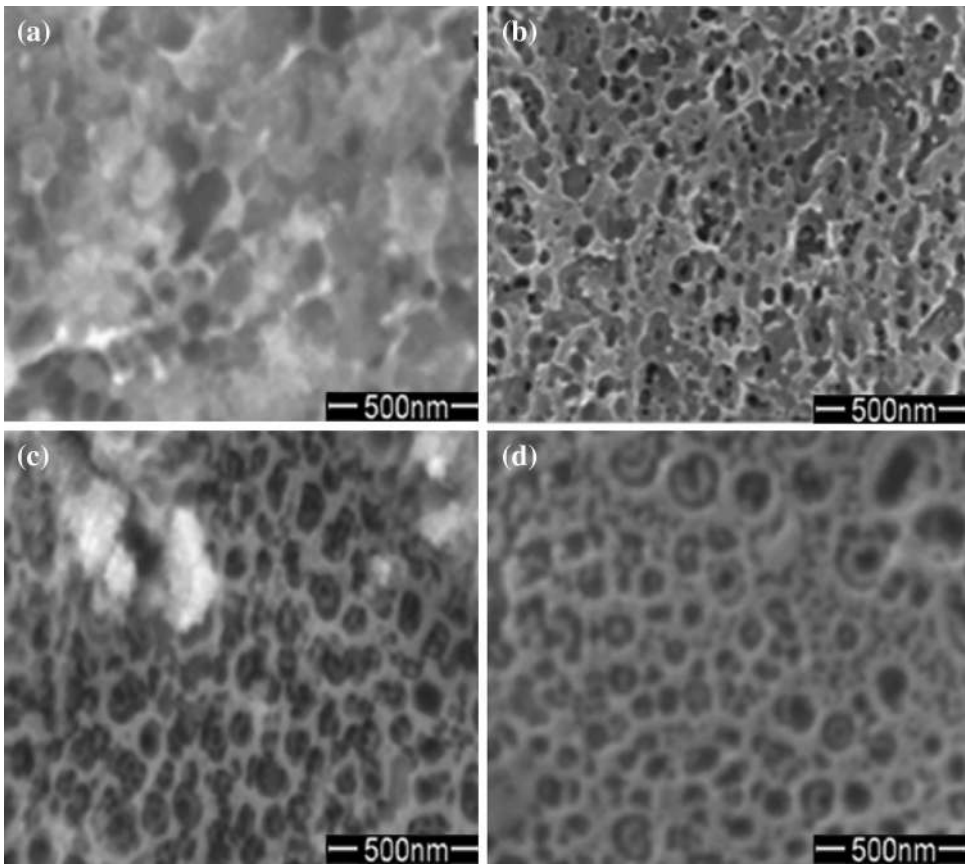

Fig. 7 FE-SEM micrographs of the as-anodized Ti samples in different electrolytes (a mixture of 0.13 M glycerol and 0.15 M HF) temperature: **a** 5 °C, **b** 10 °C, **c** 15 °C and **d** 20 °C

anodization time goes beyond 1 h, the tubes were collapsed partially due to the over dissolution of the tubes at the top by fluoride ions [163, 164].

2.7 Effect of Electrodes

In addition to the aforementioned parameters, counter electrode (CE) material used in the anodization process also influences the formation of TNT; different CEs produce different aspect ratio nanotubes. Sreekantan et al. [167] developed TNT using different kinds of CEs such as iron, carbon, stainless steel, and aluminum. They found that the TNT produced using stainless-steel cathode is short and having thin (5–10 nm), non-uniform walls thickness, and their diameter seems to vary non-uniformly at the top and bottom, which results in conical shaped TNT. At this thickness, the walls cannot support themselves, and thus collapse in unstable regions. The aspect ratio obtained using an aluminum cathode is identical to that obtained using a carbon cathode. However, the top surface of the TNT obtained using the aluminum cathode is similar to that obtained using a stainless-steel cathode. The walls at the base of these TNTs seem to be stable but the top tends to collapse. The TNT formed using an aluminum cathode is much less stable than those obtained using a carbon cathode. When an iron cathode is used, well-organized TNT is formed with high aspect ratios. However, they are less stable than those produced using a carbon cathode. Using a carbon cathode produces nanotubes with higher aspect ratios, larger tube diameters, and longer tubes than nanotubes produced using other cathode materials. Furthermore, a carbon cathode produces nanotubes that are just as good as those produced using a platinum cathode and that have similar aspect ratios. However, carbon is considerably cheaper than platinum. Allam et al. [168] used wide variety of CEs including Ni, Pd, Pt, Fe, Co, Cu, Ta, W, C, and Sn for the development of TNT. Their results indicated that the nature of the cathode material plays a vital role in the appearance of surface precipitate. The over potential of the cathode is a critical factor, which affects the dissolution kinetics of the Ti anode, in turn controlling the activity of the electrolyte and morphology of the formed TNT. More the dissolved Ti in the electrolyte, the higher the electrolyte conductivity, which in turn helps to prevent debris formation. It appears that the different cathode materials led to the fabrication of different morphologies due to differences in their overvoltage within the test electrolyte. Hence, the arrangement of the cathode materials according to their stability in aqueous electrolytes is in the following order:

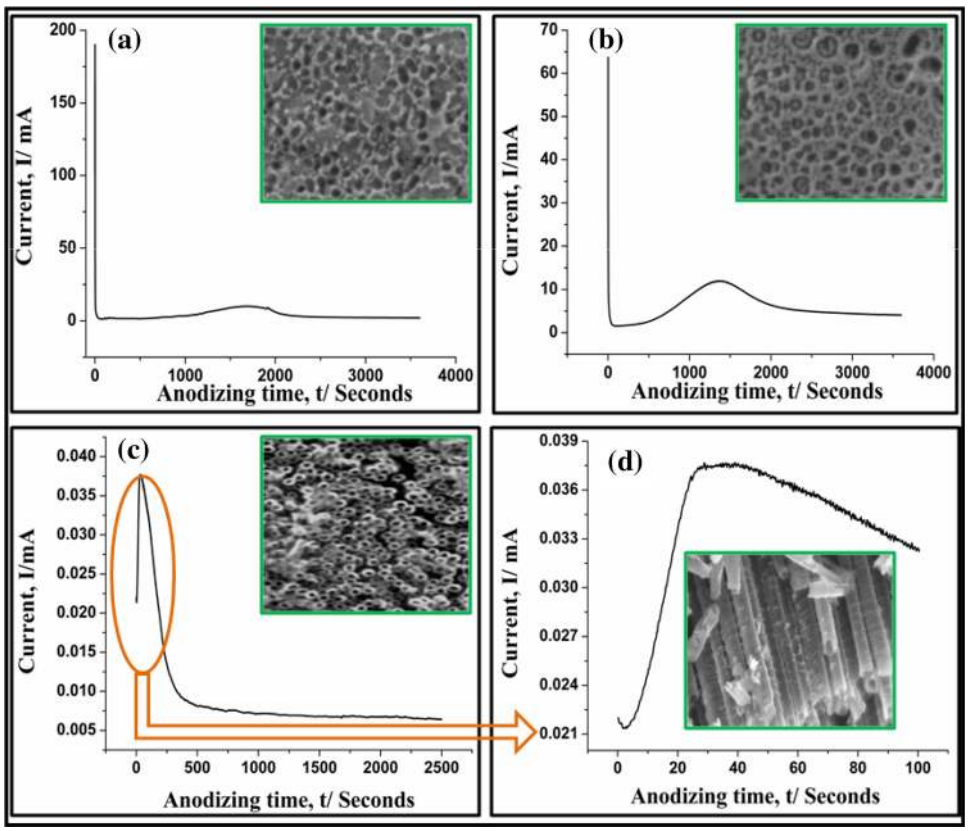

Fig. 8 Current time behavior during anodization in different electrolytes: **a** 0.13 MH_2SO_4 + 0.15 M HF, **b** 0.13 M glycerol + 0.15 M HF and (**c**, **d**) 14.5 M ethylene glycol and 0.27 M NH_4F

$$\text{Pt} = \text{Pd} > \text{C} > \text{Ta} > \text{Al} > \text{Sn} > \text{Cu} > \text{Co} > \text{Fe} > \text{Ni} > \text{W}$$

Apart from the nature of electrodes, the distance between working electrode (WE) and CE also influences the morphology of TNT. How the distance between WE and CE affects the change in electrolyte properties and corresponding morphological features of TNT is experimented by Yoriya [169]. Enlargement of pore diameters, wall thickness, and inter-tubular spacing could be achieved by simply reducing the inter-electrode spacing under a fixed condition. The electrolyte conductivity and titanium concentration were found to strongly depend upon the electrode spacing, with the closer electrode spacings reflecting high conductivity and high titanium concentration. Electrolyte conductivity and titanium concentration are found to drastically increase with decreasing anode–cathode separation. Resulting TNT also tends to increase significantly, particularly observed in inter-tubular spacing as reducing the electrode spacing from 4.5 to 0.5 cm under a fixed electrolyte condition. Due to the combination effect of electrolyte properties and high field strength between the electrodes, the self-enlargement potential is believed to be a driving force for nanotube separation. The unique characteristic of discrete, well-separated nanotube structure is expected to extend and enhance the applications of TNT. While for the case where the CE is far removed from the WE, a significant decrease in pore size and a large increase in number of TNT are obtained. The apparent decrease in pore diameter is probably due to the significant IR drop along the current path in the electrolyte reducing the field strength at the anode electrode. The growth rate of the TNT decreases with increase in the electrode distance.

3 Formation Mechanism of TNT

Figure 9 gives the FE-SEM micrographs of the TNT. After anodization, nanotube arrays (Fig. 9b) with the average diameter and wall thickness of 110 ± 4 and 15 ± 2 nm, respectively, were obtained. It is clear from Fig. 9c that the tube structures were formed with a length of approx. 2.1 ± 0.3 μm. From Fig. 9a, d, it is apparent that the tube mouth was open at the top and closed at the bottom. The average inter tube diameter (distance between the center of the adjacent tubes) was found to be 128 ± 2 nm [115]. Consequently, a detailed mechanism involved in the formation process of TNT is discussed below.

During anodization, the color of the TiO_2 layer changes from dark purple to blue, yellow, and green swiftly [170]. The color change is due to increase in the thickness of TiO_2. The formation mechanism of porous titania is similar to

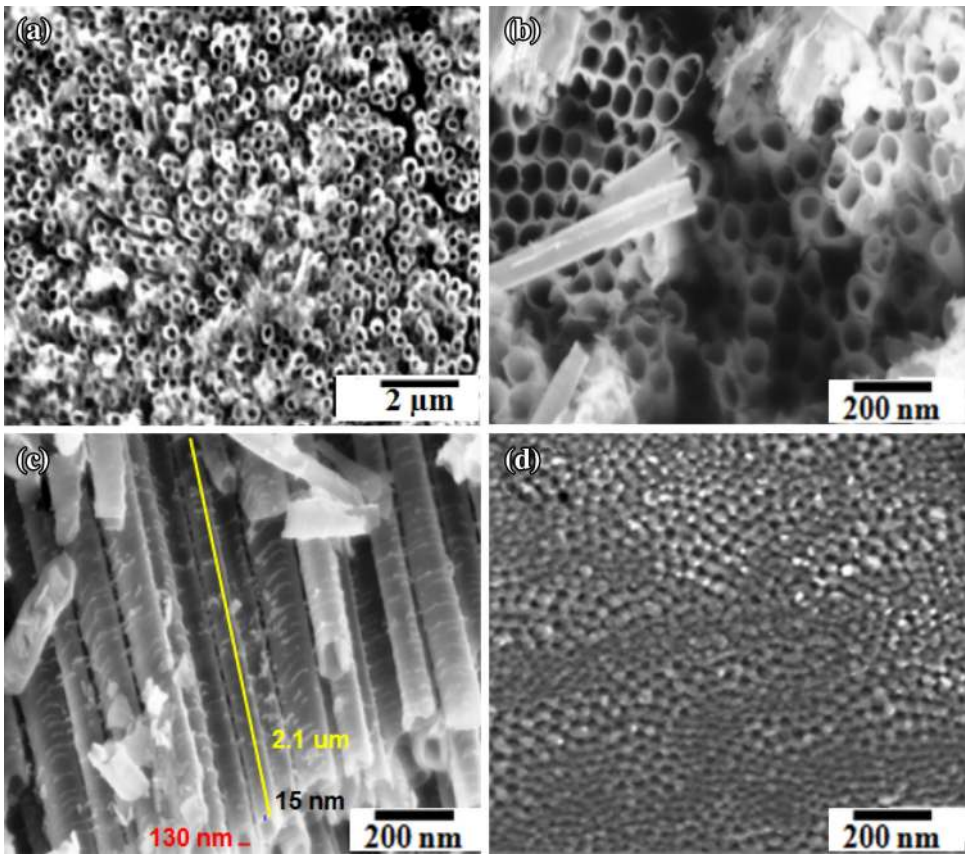

Fig. 9 FE-SEM micrographs of TNT (**a**, **b**) *top view*, (**c**, **d**) *cross-sectional view*, **e** *bottom view* and **f** EDS spectrum

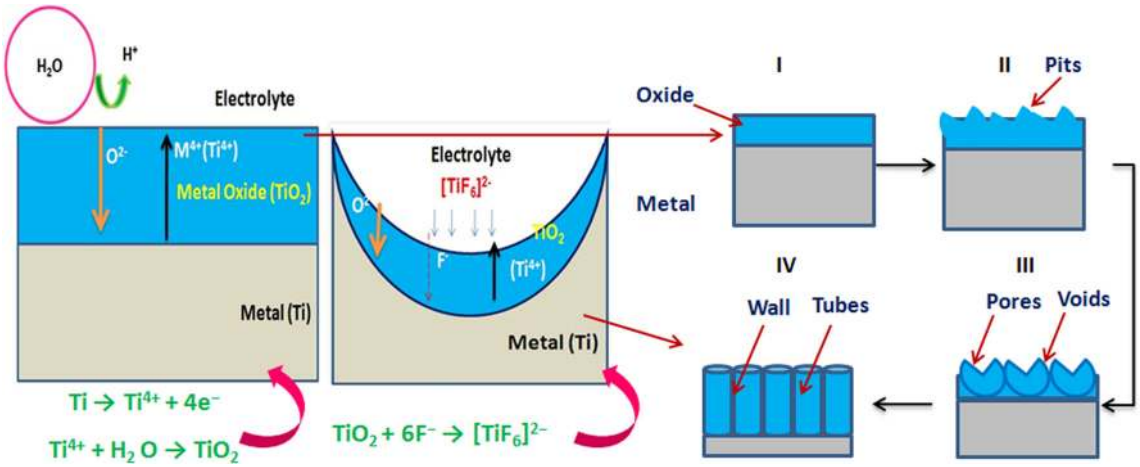

Fig. 10 Schematic illustration of formation mechanism of TNT

porous anodic alumina and silicon [171]. Presence of chloride (Cl^-) and bromide (Br^-) ions caused severe pitting corrosion and when pitting occurred, porous anodic oxide cannot be observed. Fluoride ions (F^-) are necessary for the formation of porous anodic film [172]. Figure 10 presents the schematic representation of the formation mechanism of TNT. Fluoride ion (F^-) is an essential factor for the formation of tubular structure because of its ability to form soluble hexafluoro titanium complex ($[TiF_6]^{2-}$). In addition, it has small ionic radius that makes them suitable to enter into the growing TiO_2 lattice and transported through the oxide by applied field. Simply, it acts as an oxide dissolution agent. The reactions involved in the formation of tubular nanostructure are given below [95, 173].

Oxidation of Ti

$$Ti \rightarrow Ti^{4+} + 4e^{-} \quad (1)$$

Formation of oxide layer

$$Ti^{4+} + 2H_2O \rightarrow TiO_2 + 4H^{+} \quad (2)$$

Dissolution of oxide layer

$$TiO_2 + 6F^{-} + 4H^{+} \rightarrow [TiF_6]^{2-} + 2H_2O \quad (3)$$

The Eq. 1 indicates the oxidation of Ti into Ti^{4+}. According to Eq. 2, H^+ ions accumulated during hydrolysis, F^- ions would migrate to the sites of H^+ for electroneutrality, and further, F^- ions could compete for the sites of O^{2-} in the oxide. When concentration of these ions reached a critical level at local regions, dissolution of TiO_2 occurred by the formation of $[TiF_6]^{2-}$ (Eq. 3). Dissolution of Ti could create negatively charged cation vacancies at the oxide and would migrate to the metal/oxide interface due to the potential gradient across the oxide. Presence of metal cation vacancies near the metal/oxide interface would facilitate the reaction (Eq. 1) and the Ti^{4+} could easily jump to the available vacancy sites; this was marked by rise in current (Fig. 7). During this state, nanopores were nucleated on the oxide surface [174–176], which is shown schematically along with current–time transient in Fig. 11.

Since the initial small pores are very narrow, a mass of H^+ ions are generated at the bottom of the pore, where the Ti came out of the metal and dissolved in the solution and the concentration of HF inside the pores increases rapidly. High concentration of HF makes the wall of pores dissolves until the adjacent pore walls disappear. At the same time, the integration by small pores resulted in the appearance of larger pores [174]. Simultaneously, the enhanced electric field-assisted dissolution at the pore bottom leads to deepening of the pore and the voids starts forming. Due to the applied electric field, the Ti–O bond undergoes polarization and weakened which promotes the dissolution of the metal oxide [177].

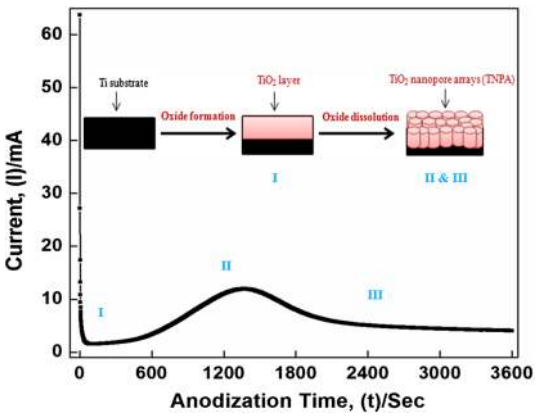

Fig. 11 Schematic illustration of nanopore formation versus current–time transient

The formation of ordered film is mainly dictated by the potential distribution at the Ti surface. Two adjacent pores tend to drifting together until the conductive Ti phase between them is not oxidized, once the metal phase is oxidized, the thickness of the oxide layer increases and the strength of the electric field in barrier layer drastically decreases, which resulted in the decrease in the migration rate of O^{2-} ions through the film. On the other hand, the diffusion lengths of O^{2-} are nearly equal for all pores and the structure tends to form a spatially ordered array with maximal packing density [178]. In summary, the mechanism of TNT formation consists of the following steps (shown in Fig. 10): (a) formation of oxide layer, (b) pore formation and deepening of the pore, (c) incorporation of adjacent small pores into a big pore, (d) earlier nanotube arrays formation, and (e) formation of perfect nanotube arrays [55].

4 Properties OF TNT

4.1 Phase Structure

The structure of the as-grown TNT is amorphous or crystalline, and this is strongly dependent on the specific electrochemical parameters such as applied potential, anodization time, and/or the sweep rate of the potential ramp. For example, the structure of the oxide films on Ti has typically been reported to be amorphous at low voltages; crystallization takes place at higher voltages [179]. Depending on the anodizing conditions, the crystal structure has been reported to be anatase [180], mixture of anatase and rutile [181], or rutile [182].

Mostly, the as-formed TNT has an amorphous structure [183–185]. Several studies have shown that the amorphous phase of tubes can be converted into anatase phase at higher temperatures (at 280 °C) in air [183] or a mixture of anatase and rutile [61, 186] at temperatures higher than 450 °C. It has also been reported that under certain conditions, nanocrystallites were present in the as-formed tubes [18].

The TNT obtained directly after anodization is amorphous and not photoactive. Therefore, it is necessary to transform the amorphous TNT into crystalline form of TNT for the use in a wide range of applications. High-temperature annealing has been regarded as an effective route to induce crystalline formation of the as-prepared TNT, converting them into anatase or rutile phase [187]. To convert the amorphous tube into crystalline anatase or rutile phase, usually annealing is necessary, because

annealing operations at several hundred degree Celsius are necessary after the anodization process. A large amount of energy is consumed in the formation of the crystalline TNT on lower thermostability material substrates [188].

Nanotubular integrity is maintained at annealing temperature lesser than 600 °C, whereas annealing in air for 3 h at a higher temperature (greater than ≥600 °C) resulted in collapse of nanotube bundles. The rutile phase emerges near 480 °C. Above this temperature, the anatase phase gradually transforms into rutile phase. At 700 °C, the amorphous Ti becomes suppressed and transforms to crystalline Ti [189, 190]. Moreover, annealing at 700 °C favors sintering and tends to destroy nanostructures completely. It is also reported elsewhere that nanotube structure was found to be stable up to approximately 550 °C. Above this temperature, nanotubes start collapsing and are destroyed [191]. Jaroenworaluck et al. [192] also reported similar observation at 600 °C. Hence, annealing temperature influences on the resistance of the nanotube structure, the annealing temperature increases the resistance of the nanotube decreases. The anatase tubes show considerably lower resistance than rutile containing tubes. Long-time annealing shows significant decrease in resistance [193]. After calcinations at 400 °C, TNT powder (prepared through rapid break down anodization) lost their tubular morphology and became spherical nanoparticles with the crystallites size of approximately 10–20 nm [194].

Some studies reported that the as-anodized TNT species exist slight anatase phase, which may due to the following reasons: (1) the outward migration of Ti^{4+} from the substrate and inward migration of O^{2-}/OH^{-} to form crystalline oxide in a ratio that favors crystal growth, (2) the internal stress relaxation of the oxide and the tube wall became thinner by dissolution after long-time anodization, and (3) faster ion mobility in the more water containing electrolyte can offer adequate ions that favor crystal growth [190]. Higher voltages can promote the crystal phase transformation spontaneously without the application of heat treatment [195].

Annealing not only influences the phase change, but it as well affects the morphology of TNT. It is reported by Lim et al [196] that there were no changes in the morphology of TNT up to the annealing temperature of 500 °C. At the annealing temperature of 600 °C, a slight decrease in the diameter and length and an increase in the wall thickness were observed. The wall thickness of TNT increases after the annealing process, which is due to the growth of crystallite on the walls. Generally, the nanostructured TNT with high surface area is thermodynamically metastable, which is prone to solid-state sintering at higher annealing temperatures. This subsequently led to grain growth, densification, and increase in the tube wall thickness [197]. Since sintering is an activated process involving mass transfer process, a higher annealing temperature and/or prolonged annealing process favor more sintering, which led to complete destruction of TNT structures [198]. In other words, the change in the morphology of TNT with annealing temperature could be associated with the excessive Ti ion diffusion along the tube walls, which induces the oxidation, and thus thickens the tube wall thickness [167, 199].

4.2 Wettability of TNT

The water contact angle of a biomaterial is a complex issue and can be affected by many factors, such as the manner of surface preparation, surface roughness, surface compositions, and chemical states [41, 42].

Figure 12 shows the contact angle image of TNT which showed super wettability for TNT [121]. The hydrophilic nature of the TNT was attributed to the capillary effect of the nanotubes [200]. Due to the capillary effect, the water droplet was sucked quickly into the pores of the tubes which caused the contact angle to be reduced dramatically [200]. Zeng et al [201] developed TNT using a mixture of H_3PO_4 and NaF. They have observed the contact angle of 4° for TNT in oil droplet. Improved wettability, i.e., low contact angle, leads to high surface energy, which is one of the key factors in better cell adhesion process.

Brammer et al. [202] developed TNT with different diameters such as 30, 50, 70, and 100 nm. They found that the contact angle reduces by increasing the tube diameter, i.e., the contact angle was found to be 11, 9, 7, and 4 for 30, 50, 70, and 100 nm diameter tubes, respectively. This is

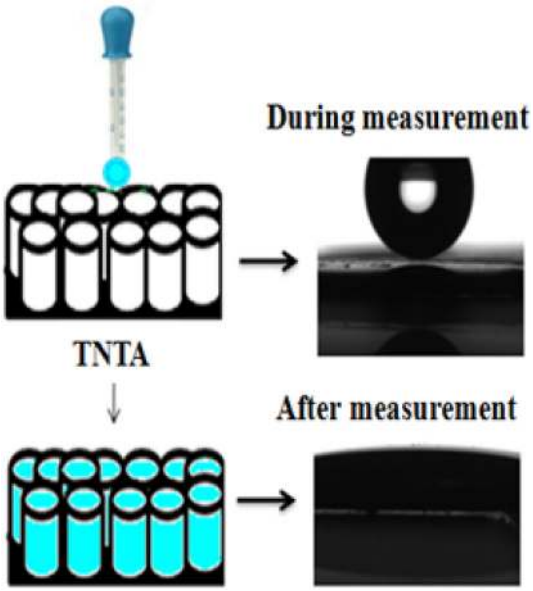

Fig. 12 Demonstration of contact angle measurements—covering of water droplets over TNT surface

due to the fact that higher the diameter of the tubes, higher the absorbance of the liquid. Similarly, Narayanan et al. reported that the water wetting angles (hydrophilic nature) increased with pore diameters which will have an important consequence on the adhesion of cells to the nanotube containing surface. Cells tend to attach better to hydrophilic surfaces than to hydrophobic surfaces [203].

It is reported elsewhere that the anodization voltage was found to have a strong effect on the resulting contact angle; at the applied voltage of 25 V, the contact angle was found to be 41.4°, whereas at the voltage of 40 V, the contact angle was increased to 13.8°. Also,, the contact angle for the freshly prepared electrolyte was found to be 51.9°, while the used electrolyte led to the highly increased contact angle with the value of up to 95.0° ± 14.8°, which clearly indicating the very low wettability of the film [149]. The nano/micro interface displayed a considerable hydrophilic property; the water contact angle (CA) was only 23.3° ± 7.9°. Thus, this hydrophilic surface is better for blood adsorption than a hydrophobic surface. It is well established from the literature that the as-formed TiO_2 surface is often partially hydroxylated and is therefore of a polar nature, which leads to relatively small advancing contact angles. In addition, the TiO_2 parameter would become dominant for very hydrophilic surface, which should contain a high number of Lewis acidic Ti–OH groups [204].

In addition, crystalline phase of TNT also plays a vital role in the surface wettability. Recently, Munirathinam et al. [205] reported that similar to the amorphous TNT, the annealed TNT also exhibited hydrophilic nature, which is mainly due to the presence of mixed crystalline phase (anatase and rutile). The hydrophilic behavior of amorphous TNT could be attributed to the density of hydroxyl group on their surface and the high polarity of O–Ti–O bond. Up to the annealing temperature of 450 °C, the TNT surface is super hydrophilic, when the annealing temperature was further increased, the hydrophilic nature started to decrease. This is because of the lack of hydroxyl group on the surface of TNT after annealing at higher temperatures (above 450 °C). The surface hydroxyl can easily combine with water molecule, thus, formed hydrogen bond resulting in good wettability [206].

4.3 Surface Roughness

Generally, biologically active implant materials have enhanced surface roughness, which was one of the important factors in providing better cell response to implanted materials [207]. Lu et al. [208] studied the effect of the surface roughness on the TNT formation during the anodization, which showed that the nanotubes formed from the as-received and chemically polished samples have rough surfaces, as a result, the corresponding nanotube morphology and bottom oxide barrier layer are non-uniform.

The average surface roughness of TNT prepared using ethylene glycol and ammonium fluoride electrolyte was found to be 360 nm [115]. Anodization increased the surface roughness by forming a porous layer on Ti surface. It has been reported elsewhere that the surface roughness of TNT with the diameter of 30, 50, 70, and 100 nm was 13, 12.7, 13.5, and 13.2 nm, respectively [149]. This result confirmed that the tube diameter has not played any role in altering the surface roughness of the TNT. It is reported elsewhere that the TNT showed nanorough (12.62 nm) surface and the anodization process did not create micro-topographical differences, whereas it did create nanotopographical differences [49].

The inter-tubular spacing in the TNT has significant influence on the surface roughness [209]. Annealing not only influences the phase change, but it as well affects the lateral spacing between the TNT which is attributed to the crystallization and crystal growth [210]. It is reported by Lim et al. [196] that there were no changes in the morphology of TNT up to the annealing temperature of 500 °C. A slight increase in the wall thickness (laterally attached together), in other words, a decrease in the lateral spacing was observed at the annealing temperature of 600 °C. The lateral spacing of TNT decreases after the annealing process, which is due to the growth of crystallite on the walls. Generally, the nanostructured TNT with high surface area is thermodynamically metastable, which is prone to solid-state sintering at higher annealing temperatures. This subsequently led to grain growth, densification, and decrease in the lateral spacing [197]. In addition, annealing at higher temperature leads to the formation of barrier layer between the tubes and the underlying Ti substrate [211]. In other words, decrease in the lateral spacing of TNT with annealing temperature could be associated with the excessive Ti ion diffusion along the tube walls, which induces the oxidation, and thus thickens the tube wall thickness, i.e., decreases the lateral spacing [167]. Besides, the distance between the WE and CE also influences the inter-tubular spacing, which was already discussed in the previous section (Sect. 2.7).

5 Biomedical Applications

According to many researchers, the TNT might be used in drug-eluting stents and for the local release of antibiotics [44], drugs, or growth factors from orthopedic and dental implants [212]. Hence, this section provides the detailed information of TNT in the biomedical field.

5.1 As Orthopedic and Dental Implants

A common treatment for bone fracture is the implantation of a mostly metallic orthopedic prosthetics. These prosthetics help in healing bone non-unions and allow patients to partially regain their function. However, today's orthopedic implant materials do not allow patients to return to their normal, daily active lifestyles that they had before fracture. Specifically, it has been reported that the average lifetime of orthopedic implants is only 10–15 years. This means that those who are young and receive a traditional orthopedic implant will have to undergo several more painful and expensive revision surgeries to replace such a failed orthopedic implant. Although controversial several factors such as incomplete, prolonged osseo-integration (i.e., lack of bonding of an orthopedic implant to juxtaposed bone) and severe stress shielding (due to differences in mechanical properties between an implant and the surrounding bone) lead to implant failures [213]. Therefore, a great amount of efforts from biomedical researchers worldwide have given on improving the design and manufacture of orthopedic implants to last longer in the body. While many have attempted to alter orthopedic implant chemistry (from metals to ceramics to polymers), recent discoveries have highlighted that nanotechnology may universally improve all materials used for re-growing bone. The use of nanostructured materials has been proposed to solve some of the problems currently associated with orthopedic implants [123].

As a biocompatible material, Ti and its alloys are extensively used in orthopedic and dental implants mainly because of its optimal mechanical properties in load-bearing applications [214]. However, insufficient new bone formation is frequently observed on Ti which sometimes leads to implant loosening and failure. For this reason, TNT with good bioactivity has been developed by anodic oxidation which may be a simple method to modify the surface of Ti implants to enhance bone-forming function, thereby increasing orthopedic implant efficiency [215]. There have been several studies [216, 217] reported on TNT for bone tissue engineering applications.

The presence of HAp coating promotes osteo-conduction. Surface treatments such as roughing by sand blasting, formation of anatase phase TiO_2, HAp, and $Ca_{10}PO_4{\cdot}2H_2O$ coating have been utilized to further improve the bioactivity of Ti and enhance bone growth. Heat-treated TNT, when soaked in simulated body fluid (SBF) solution is completely covered with HAp layer, and thereby provides excellent bioactivity [46]. It is well established that the anatase phase TiO_2 is much more efficient in nucleation and growth of HAp than the rutile phase TiO_2 presumably because of the better lattice match with HAp phase. The formation of bone growth-related material such as the calcium-phosphate HAp is an important issue for orthopedic and dental implants. Bone is a calcium-phosphate-based mineral which contains ~70 % HAp-like material with remainder consisting mostly of collagen [218].

Treating TNT with NaOH solution induces the growth of nanosized HAp when subjected to SBF. Furthermore, nanophase ceramics such as HAp, Al_2O_3, and TiO_2 enhance long-term osteoblast functions relative to typical microstructure forms. Thus, the HAp forming and bone-bonding ability of Ti bone implant materials may be significantly enhanced by anodically oxidized nanotubes on the surface of Ti [219]. The TNT is adherent well to Ti implant surface and can be useful for accelerated bone growth in orthopedic and dental applications. Advantage of strong mechanical adherence, the gaps present between adjacent TNT, may also be useful as a pathway for continuous supply of the body fluid with ions, nutrients, and proteins. This is likely to continue positively to the health of the growing cell [220, 221]. The TNT with Ca was also developed, where it was used for bone repair in filling defective areas of bones. Newly formed bone was found around TNT with Ca surface after being implanted in the femur of a rat for 7 days. This phenomenon indicated that Ca-TNTs induced excellent bone tissue regeneration at implantation [222]. Very low adhesion strengths were reported for electrochemically produced HAp coatings. Plasma-sprayed HAp coating has also been reported to have tensile adhesion strengths lower that 10 MPa, and their heterogeneous structure was reported to cause poor adhesion. Poor adhesion of TNT is attributed to the stirring condition of the electrolyte [144].

5.2 As a Corrosion-Resistant Materials

The TNT layers, formed on Ti surfaces, are highly suitable host for synthetic HAp coating deposited by an alternative immersion method (AIM) [223]. In our earlier report, we have developed nanoporous titania and observed their corrosion behavior for the use of orthopedic implant application. The nanoporous titania after immersion in Hank's solution for 7 days showed excellent bioactivity and corrosion resistance than the untreated Ti, which was attributed to the growth of HAp layer on their surface [224]. In addition, our previous studies showed the incorporation of Sr [115] and Zr [117] into TNT for the use of orthopedic implant. Figure 13a–c shows the polarization curves of TNT and TNT with Sr and Zr ion after immersion in Hank's solution for immediate, 3, 5, and 7 days. The results showed that the TNT with Sr and Zr ions showed enhanced corrosion resistance than the TNT without Sr and Zr which attributed to the formation of thick HAp layer on the TNT surface [225]. The presence of Sr and Zr ions on the TNT surface facilitates the growth of HAp with less

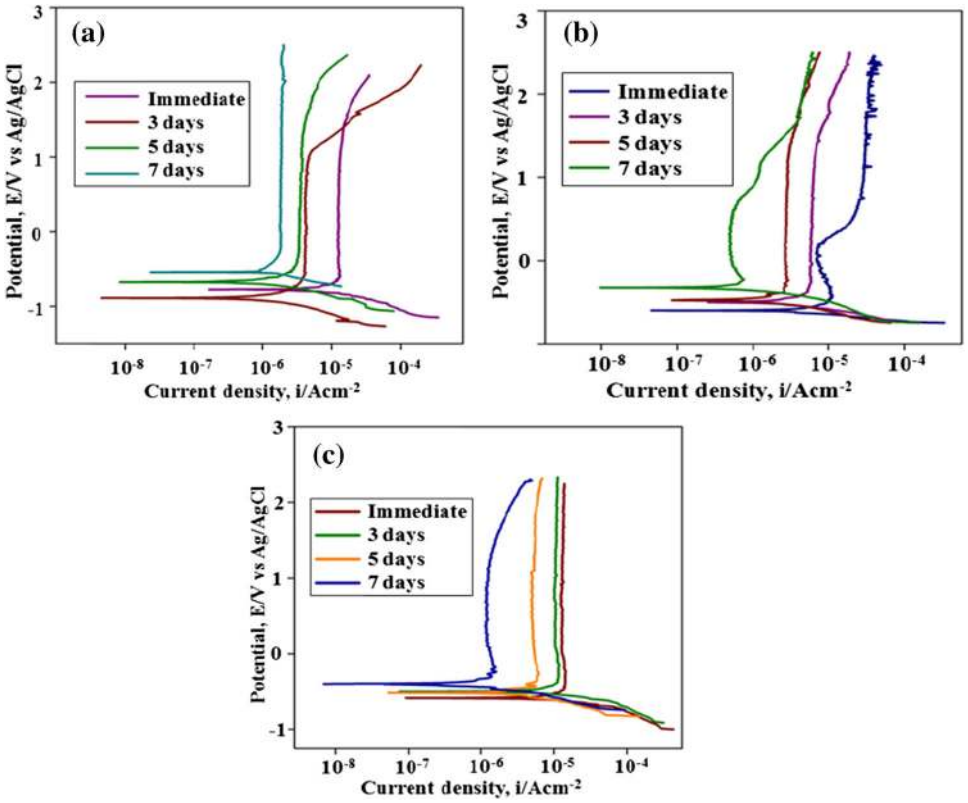

Fig. 13 Polarization curves of **a** TNT, **b** TNT with Sr and **c** TNT with Zr after immediate, 3, 5, and 7 days of immersion in Hank's solution

time, which in turn enhances the corrosion resistance. Recently, Parcharoen et al. [226] coated HAp on TNT by electrodeposition method. The HAp-coated TNT showed higher cells density, higher live cells, and more spreading of MC3T3-E1 cells than the untreated Ti implants. Huang et al. [227] found that the TNT developed on 316L stainless-steel substrate gives improved corrosion resistance and hemocompatibility for stainless-steel implants. The materials, which have both reducing platelet adhesion and improving corrosion resistance, can be used as a permanent biomaterial in blood contacting biomedical devices. Recently, we have developed nanotube arrays on Ti–6Al–7Nb alloy, nitrided the TNT in a nitrogen plasma, and the corrosion behavior was observed in a Hank's solution for the biomedical applications [228]. Plasma nitriding increases the biocompatibility and decreases the corrosion resistance of the TNT.

5.3 As Blood Clotting and Anti-microbial Agent

The blood and tissue compatible coatings on surgical tools as well as artificial bone and dental implants are of paramount importance. The TiO_2 helps to retain the natural forms of proteins and also minimize unwanted platelet activation due to its passive surface and chemical stability. The TNT is used as an adhesion and growth support platform for bone and stem cells [229, 230]. Gauze bandage surfaces decorated with TNT could be used to improve the rate of blood clot formation and the strength of the resulting clot [45].

Silver (Ag)-doped TNT has good biological applications. However, Ag is probably the most powerful antimicrobial that exhibits strong cytotoxicity toward a broad range of micro-organisms and remarkable low human toxicity compared to other heavy metal ions [231]. Recently, studies on cell interaction with TNT show cell adhesion, proliferation, and migration, and are significantly affected by the nanotube size [18]. The TNT can improve osteoblast attachment, function, and proliferation. Furthermore, these surfaces also exhibit very low immunogenicity, eliciting low levels of monocyte activation, and cytokine secretion [232]. Others [233, 234] suggest that nanotubes are also used in vascular applications, enhancing endothelial cell ECM production and mobility. Recently, Lan et al. [235] decorated the TNT with Ag by e-gun vacuum evaporation system and studied the influence of tube diameter on human nasal epithelial cell. The results showed that the Ag-coated TNT with the diameter of 25 nm revealed antibacterial effect against *P. aeruginosa*.

5.4 In Cancer and Tumor Therapy

Most recently, researchers found that the TNT is a potential drug delivery vehicle in nanomedicine, which is used as a

nanovehicle for cancer drug delivery. Generally, nanotubes have significant advantages over nanoparticles in a medicine carrier. In contrast to the spherical nanoparticles, the geometry of nanotubes must allow them to be multiply functionalized by different molecules that allow the nanovehicle to carry the drug more efficiently to target for the purpose of cancer therapy. The exploration of nuclear DNA-targeting nanotubes carrying anti-tumor drugs is of particular importance. Undoubtedly, it is one of the difficult challenges in the emerging area of cancer nanotechnology. The TNT is able to cross karyotheca and enter the nucleus, hence, it is a promising future nanovehicle for DNA-targeting drugs in cancer therapy [236, 237].

The self-organized, highly ordered tubular architecture of anodic TNT has been shown to be an excellent substrate for adherence, spreading, and growth of living cells, which promote cellular activity. When the tube morphological characteristics are approximately tuned, most importantly, the anodic TNT can act as efficient photocatalysts for the photo-induced killing of cancer cells [107]. The dimensions of the nanotubes play a vital role for cell adhesion and spreading. A possible application of the nanotubes may be anticancer treatment, where isolated tubes are administrated to a tumor, followed by a focused UV-light exposition of the tumor [238]. Chen et al. [239] incorporated selinium and chitosan onto TNT for the anticancer treatment. The results indicated that TNT with selenium and chitosan substrates promoted the biological functions of healthy osteoblasts and inhibited the growth of cancerous osteoblasts. More importantly, in vitro antibacterial assay revealed that the TNT with selenium and chitosan substrates had good antibacterial property.

5.5 In Drug Delivery

In recent years, controlled drug delivery applications have gained increasing attention and the rapid expansion in the advanced materials, and technology has resulted in a remarkable progress in their development. The TiO_2 is a good candidate for drug-eluting implant coating as it is highly biocompatible and able to control protein and antibiotic [240]. Benefiting from large surface area, excellent biocompatibility, and one-end open feature, the TNT has been applied in drug delivery [241, 242]. A large number of implants in dentistry and orthopedics are made from Ti alloys, and the possibility of using TNT to deliver drugs and other compounds from these implants appear to be quite attractive. Local delivery of drug from an implant surface may be desirable as it can reduce the amount of drug requirement and may also reduce the systemic side effects.

Moseke et al. [243] reported that the TNT can be used as a long-term drug delivery system for anti-microbial agents. It has been reported elsewhere that the chemical functionalized groups may act as an inbuilt regulator for achieving different drug dosages. Modulation of surface chemistry and kinetics of TNT alters both the morphological parameters (e.g., surface area and pore dimensions) and the drug loading percentages. The loading amount gets reduced with hydrophobic surface, whereas it increases with hydrophilic moieties. This in turn influences the release rates, thus, varying from fast release with hydrophobic functionalization to very slow release with hydrophilic functionalization. These chemical functionalized groups may act as an inbuilt regulator for achieving different drug dosages. The main driving force for the drug encapsulation arises from hydrogen bond interaction between the drug molecule and the –OH groups present in the pore walls of TNT. Given that the drug and pore wall interaction are high, the release rate is low and vice versa. If the surface of TNT is modified with the hydrophobic groups like $–CH_3$ and impregnated with drugs like ibuprofen, the interaction between the drug and the tube walls gets decreased leading to low loading percentage, which in turn increases the release rate of drug [244].

It has been reported that the nanotube height and the loading solution concentration have more influence on drug release, whereas the crystalline structure of the nanotubes does not influence the amount of drug released [245]. It has also been reported that the TNT could maintain the bioactivity of the loaded drug and dictate the biological responses of mesenchymal stem cells [246]. Wang et al. [247] developed TNT with P25 nanoparticles for the effective delivery of ibuprofen drug. They found that the TNT with P25 nanoparticles could improve the drug adsorption capacity and sustained release of drugs. The TNT with biodegradable polymers like chitosan and PLGA has extended drug release property, biocompatibility for human osteoblasts, and potentially improved antibacterial properties. This kind of polymer-modified TNT is capable of delivering the drug to a bone site over an extended period with predictable kinetics [248].

6 Conclusions

In this article, we reviewed the synthesis, formation mechanism, various parameters, which affects the tube formation mechanism and properties of TNT and their wide range of applications in the biomedical field. The tube length, thickness, and diameter were varied according to the pH, electrolytes, anodization potential, and time. The as-prepared nanotubes have amorphous structure and can be transformed into crystalline by annealing at higher temperature. The crystalline nanotubes were often used for the bio-implant application purposes. Today, nanotubes are

used as orthopedic and dental implants, blood clotting, and anti-microbial agents and also used as an effective drug delivery vehicle for the cancer therapy. By using the TNT, the field of nanomedicine has a bright future with the emergence of several promising approaches for drug delivery and cancer treatments.

Compliance with Ethical Standards

Conflict of Interest There is no conflict of interest in this article.

References

1. Peighambardoust NS, Nasirpouri F (2013) Manipulating morphology, pore geometry and ordering degree of TiO_2 nanotube arrays by anodic oxidation. Surf Coat Technol 235:727–734
2. Murday JS, Seigel R, Stein J et al (2009) Feature article: preclinical nanomedicine, review translational nanomedicine: status assessment and opportunities. Nanomed Nanotechnol Biol Med 5:251–273
3. Roco MC (1998) Reviews of National Research Programs in Nanoparticle and Nanotechnology Research. J Aerosol Sci 29:749–760
4. Murday JS (2002) The coming revolution: science and technology of nanoscale structures. AMPTIAC Newslett. Spring 6:1
5. Xiao P, Zhang Y, Garcia BB et al (2008) Nanostructured electrode with titania nanotube arrays: fabrication, electrochemical properties, and applications for biosensing. J Nanosci Nanotechnol 8:1–11
6. Zhao J, Wang X, Li L (2005) Electrochemical fabrication of well-ordered titania nanotubes in H3PO4/HF electrolytes. Electron Lett 41:13
7. Yue C, Chuan MD, Bin ZH et al (2009) Pool boiling on the superhydrophilic surface with TiO_2 nanotube arrays. Sci China-Ser E: Technol Sci 52:1596–1600
8. Costa LL, Prado AGS (2009) TiO_2 nanotubes as recyclable catalyst for efficient photocatalytic degradation of indigo carmine dye. J Photochem Photobiol A Chem 01:45–49
9. Liang HC, Li XZ (2009) Visible-induced photocatalytic reactivity of polymer-sensitized titania nanotube films. Appl Catal B 86:8–17
10. Whang TJ, Huang HY, Hsieh MT et al (2009) Laser-induced silver nanoparticles on TiO_2 for photocatalytic degradation of methylene blue. Int J Mol Sci 10:4707–4718
11. Liu S, Smith YR, Misra M et al (2009) Photocatalytic activities of C-N-doped TiO_2 nanotube array/carbon nanorod composites. Electrochem Commun 11:1748–1751
12. Sohn YS, Smith YR, Misra M et al (2008) Electrochemically assisted photocatalytic degradation of methyl orange using anodized titanium dioxide nanotubes. Appl Catal B 84:372–378
13. Sun L, Li J, Wang CL et al (2009) An Electrochemical strategy of Doping Fe^{3+} into TiO_2 nanotube array films for enhancement in photocatalytic activity. Sol Energy Mater Sol Cells 93:1875–1880
14. Xie YB, Li XZ (2006) Preparation and characterisation of TiO_2/Ti film electrodes by anodization at low voltage for photocatalytic application. J Appl Electrochem 36:663–668
15. Li H, Zhu B, Feng Y et al (2007) Synthesis, characterisation of TiO_2 nanotubes-supported MS (TiO_2 NTs@MS, M = Cd, Zn) and their photocatalytic activity. J Solid State Chem 180:2136–2142
16. Awitor KO, Rafqah S, Geranton G et al (2008) Photo-catalysis using titanium dioxide nanotube layers. J Photochem Photobiol A Chem 199:250–254
17. Paramasivam I, Avhale A, Inayat A et al (2009) MFI-type (ZSM-5) Zeolite filled TiO_2 nanotubes for enhanced photocatalytic activity. Nanotechnology 20:225607
18. Macak JM, Tsuchiya H, Ghicov A et al (2007) TiO_2 nanotubes: self-organised electrochemical formation, properties and applications. Curr Opin Solid State Mater Sci 11:3–18
19. Ghicov A, Schmuki P (2009) Self-ordering electrochemistry: a review on growth and functionality of TiO_2 nanotubes and other self-aligned mox structures. Chem Commun 20:2791–2802
20. Geng J, Jiang Z, Wang Y et al (2008) Carbon modified TiO_2 nanotubes with enhanced photocatalytic activity synthesized by a facile wet chemistry method. Scr Mater 59:352–355
21. Ghicov A, Tsuchiya H, Hahn R et al (2006) TiO_2 nanotubes: H+ incertion and strong electrochromic effects. Electrochem Commun 8:528–532
22. Liu Z, Raja BSKS, Rangaraju RR et al (2009) Hydrogen generation under sunlight by self-ordered TiO_2 nanotube arrays. Int J Hydrog Energy 34:3250–3257
23. Bae S, Shim E, Yoon J et al (2008) Enzymatic hydrogen production by light-sensitized anodized tubular TiO_2 photoanode. Sol Energy Mater Sol Cells 92:402–409
24. Narayanan R, Seshadri SK (2006) Anodic oxide coatings on Ti-6Al-4V produced from electrolyte containing Ca and P-corrosion aspects. J Appl Electrochem 36:475–479
25. Mor GK, Varghese OK, Paulose M et al (2006) A Review on highly ordered, vertically oriented TiO_2 nanotube arrays: fabrication, material properties, and solar energy applications. Solar Energy Mater Solar Cells 90:2011–2075
26. Chanmanee W, Watcharenwong A, Chenthamarakshan CR et al (2007) Titania nanotubes from pulse anodisation of titanium foils. Electrochem Commun 9:2145–2149
27. Allam NK, Grimes CA (2009) Room temperature one-step polyol synthesis of anatase TiO_2 nanotube arrays: photoelectrochemical properties. Langmuir 25:7234–7240
28. Li XD, Zhang DW, Sun Z et al (2009) Metal–free Indoline-dye-sensitized TiO_2 nanotube solar cells. Microelectron J 40:108–114
29. Varghese OK, Gong D, Paulose M et al (2008) Hydrogen sensing using titania nanotubes. Sensor Actuat B 93:338–344
30. Banerjee S, Mohapatra SK, Misra M et al (2009) The detection of improvised nonmilitary peroxide based explosives using a titania nanotube array sensor. Nanotechnology 20:075502
31. Seo MH, Yuasa M, Kida T et al (2009) Gas sensing characteristics and porosity control of nanostructured films composed of TiO_2 nanotubes. Sens Actuators B: Chem 137:513–520
32. Guo C, Hu F, Li CM et al (2008) Direct electrochemistry of hemoglobin on carbonized titania nanotubes and its application in a sensitive reagentless hydrogen peroxide biosensor. Biosens Bioelectron 24:819–824
33. Kafi AKM, Wu G, Chen A (2008) A novel hydrogen peroxide biosensor based on the immobilization of horseradish peroxidase onto Au-modified titanium dioxide nanotube arrays. Biosens Bioelectron 24:566–571
34. Xie Y, Zhou L, Huang H (2007) Bioelectrocatalytic application of titania nanotube array for molecule detection. Biosens Bioelectron 22:2812–2818
35. Zhao R, Xu M, Wang J et al (2010) A pH sensor based on the TiO_2 nanotube array modified Ti electrode. Electrochim Acta 55:5647–5651
36. Li Y, Yu X, Yang Q (2009) Review article-fabrication of TiO_2 nanotube thin films and their gas sensing properties. J Sensors. Article ID 402174
37. Pillai P, Raja KS, Misra M (2006) Electrochemical storage of hydrogen in nanotubular TiO_2 arrays. J Power Sour 161: 524–530

38. An LP, Gao XP, Li GR et al (2008) Electrochemical lithium storage of titania nanotube modified with NiO nanoparticles. Electrochim Acta 53:4573–4579
39. Zhang Z, Yuan Y, Fang Y et al (2007) Photoelectrochemical oxidation behavior of methanol on highly ordered TiO_2 nanotube array electrodes. J Electroanal Chem 610:179–185
40. Zhang J, Zhou B, Zheng Q et al (2009) Photocatalytic COD determination method using highly ordered TiO_2 nanotube array. Water Res 43:1986–1992
41. Balaur E, Macak JM, Taveira L et al (2005) Tailoring the wettability of TiO_2 nanotube layers. Electrochem Commun 7:1066–1070
42. Lai Y, Lin C, Wang H et al (2008) Superhydrophilic-superhydrophobic micropattern on TiO_2 nanotube films by photocatalytic lithogtraphy. Electrochem Commun 10:387–391
43. Crawford GA, Chawla N, Houston JE (2009) Nanomechanics of biocompatible TiO_2 nanotubes by interfacial force microscopy (IFM). J Mech Behav Biomed Mater 2:580–587
44. Popat KC, Eltgroth M, Tempa TJL et al (2007) Decreased *Staphylococcus epidermis* adhesion and increased osteoblast functionality on antibiotic-loaded titania nanotubes. Biomater 28:4880–4888
45. Roy SC, Paulose M, Grimes CA (2007) The effect of TiO_2 nanotubes in the enhancement of blood clotting for the control of hemorrhage. Biomater 28:4667–4672
46. Li MO, Xiao X, Liu R (2008) Synthesis and bioactivity of highly ordered TiO_2 nanotube arrays. Appl Surf Sci 255:365–367
47. Oh SH, Finones RR, Daraio C et al (2005) Growth of nano-scale hydroxyapatite using chemically treated titanium oxide nanotubes. Biomater 26:4938–4943
48. Sul YT, Johansson CB, Petronis S et al (2002) Characteristics of the surface oxides on turned and electrochemically oxidized pure Ti implants up to dielectric breakdown: the oxide thickness, micropore configurations, surface roughness, crystal structure and chemical composition. Biomater 23:491–501
49. Ercan B, Webster TJ (2010) The effect of biphasic electrical stimulation on osteoblast function at anodized nanotubular titanium surfaces. Biomater 31:3684–3693
50. Zhang A, Zhou M, Han L et al (2011) The combination of rotating disk photocatalytic reactor and TiO_2 nanotube arrays for environmental pollutants removal. J Hazard Mater 186: 1374–1383
51. Kilin N, Sennik E, Ozturk ZZ (2011) Fabrication of TiO_2 nanotubes by anodization of Ti thin films for VOC sensing. Thin Solid Films 520:953–958
52. Ma Q, Li M, Hu Z et al (2011) Enhancement of the bioactivity of titanium oxide nanotubes by precalcification. Mater Lett 62:3035–3038
53. Wilmowsky CV, Bauer S, Lutz R et al (2008) In vivo evaluation of anodic TiO_2 nanotubes: an experimental study in the Pig. Inc J Biomed Mater Res Part B: Appl Biomater 89B:165–171
54. Wang N, Li H, Lu W et al (2011) Effects on TiO_2 nanotubes with different diameters on gene expression and osseo-integration of implants in minipigs. Biomater 32:6900–6911
55. Zhao J, Wang X, Chen R et al (2005) Fabrication of titanium oxide nanotube arrays by anodic oxidation. Solid State Commun 134:705–710
56. Narayanan R, Lee JH, Kwon TY et al (2011) Anodic TiO_2 nanotubes from stirred baths: hydroxyapatite growth & osteoblast responses. Mater Chem Phys 125:510–517
57. Kaneco S, Chen Y, Westerhoff P et al (2007) Fabrication of uniform size titanium oxide nanotubes: impact of current density and solution conditions. Scr Mater 56:373–376
58. Tsuchiya H, Macak JM, Sieber I et al (2005) Self-organised high-aspect-ratio nanoporous zirconium oxides prepared by electrochemical anodization. Small 1:722–725
59. Biswas S, Shahjahan M, Hossain MF et al (2010) Synthesis of thick TiO_2 nanotube arrays on transparent substrate by anodization technique. Electrochem Commun 12:668–671
60. Macak JM, Tsuchiya H, Schmuki P (2005) High-aspect-ratio TiO_2 nanotubes by anodization of titanium. Nanoporous Mater 44:2100–2102
61. Mohapatra SK, Misra M, Mahajan VK et al (2007) Synthesis of Y-branced TiO_2 nanotubes. Mater Lett 62:1772–1774
62. Perillo PM, Rodriguez DF (2012) The gas sensing properties at room temperature of TiO_2 nanotubes by anodization. Sens Actuators B 171–172:639–643
63. Yang DJ, Kim HG, Cho SJ et al (2008) Thickness-conversion ratio from titanium to TiO_2 nanotubes fabricated by anodization method. Mater Lett 62:775–779
64. Lei L, Su Y, Zhou M et al (2007) Fabrication of multi-non-metal-doped TiO_2 nanotubes by anodization in mixed acid electrolyte. Mater Res Bull 42:2230–2236
65. Zlamal M, Macak JM, Schmuki P et al (2007) Electrochemically assisted photocatalysis on self-organised TiO_2 nanotubes. Electrochem Commun 9:2822–2826
66. Song H, Qiu X, Guo D et al (2008) Role of structural H_2O in TiO_2 nanotubes in enhancing Pt/C direct ethanol fuel cell anode electro-catalysts. J Power Sour 178:97–102
67. Song H, Qiu X, Li F et al (2007) Ethanol electro-oxidation on catalysts with TiO_2 coated carbon nanotubes as support. Electrochem Commun 9:1416–1421
68. Macak JM, Schmidt-Stein F, Schmuki P (2007) Efficient oxygen reduction on layers of TiO_2 nanotubes loaded with Au nanoparticles. Electrochem Commun 9:1783–1787
69. Ayala SL, Rincon ME, Pfeiffer H (2009) Influence of copper on the microstruture of sol-gel titanium oxide nanotubes array. J Mater Sci 44:4162–4168
70. Na SI, Kim SS, Hong WK et al (2008) Fabrication of TiO_2 nanotubes by using electrodeposited ZnO nanorod template and their application to hybrid solar cells. Electrochim Acta 53:2560–2566
71. Bae C, Yoo H, Kim S et al (2008) Template-directed synthesis of oxide nanotubes: fabrication, characterization, and applications. Chem Mater 20:756–767
72. Lin CH, Chien SH, Chao JH et al (2002) The synthesis of sulfated titanium oxide nanotubes. Catal Lett 80:153–159
73. Yuan ZY, Su BL (2004) Titanium oxide nanotubes, nanofibers and nanowires. Colliods Surf A Physiochem Eng Asp 241: 173–183
74. Gang L, Zhongqing L, Zhao Z et al (2009) Preparation of titania nanotube arrays by the hydrothermal method. Chin J Catal 30:37–42
75. Choi MG, Lee YG, Song SW et al (2010) Lithium-ion battery anode properties of TiO_2 nanotubes prepared by the hydrothermal synthesis of mixed (anatase and rutile) particles. Electrochim Acta 55:5975–5983
76. Wang D, Zhou F, Li Y et al (2008) Synthesis and characterisation of anatase TiO_2 nanotubes with uniform diameter from Ti powder. Mater Lett 62:1819–1822
77. Nguyen QA, Bhargava YV, Devine TM (2008) Titania nanotube formation in chloride and bromide containing electrolytes. Electrochem Commun 10:471–475
78. Tsai CC, Teng H (2004) Regulation of the physical characteristics of titania nanotube aggregates synthesized from hydrothermal treatment. Chem Mater 16:4352–4358
79. Kukoveez A, Hodos M, Horvath E et al (2005) Oriented crystal growth model explains the formation of titania nanotubes. J Phys Chem B 109:17781–17783
80. Khan MA, Yang OB (2009) Optimization of silica content in initial sol-gel grain particles for the low temperature hydrothermal synthesis of titania nanotubes. Cryst Growth Des 9:1767–1774

81. Niu L, Shao M, Wang S et al (2008) Titanate nanotubes: preparation, characterisation, and application in the detection of dopamine. J Mater Sci 43:1510–1514
82. Mohapatra SK, Misra M, Mahajan AK et al (2007) A novel method for the synthesis of titania nanotubes using sonoelectrochemical method and its application for photoelectrochemical splitting of water. J Catal 246:362–369
83. Mohapatra SK, Raja KS, Misra M et al (2007) Synthesis of self-organised mixed oxide nanotubes by sonoelectrochemical anodization of Ti-8Mn alloy. Electrochim Acta 53:590–597
84. Wang CL, Sun L, Yun H et al (2009) Sonoelectrochemical synthesis of highly active TiO_2 nanotubes by incorporating CdS nanoparticles. Nanotechnology 20:295601
85. Liu Y, Zhou B, Li J et al (2009) Preparation of short, robust and highly ordered TiO_2 nanotubes arrays and their applications as electrode. Appl Catal B Environ 92:326–332
86. Ribbens S, Meynen V, Tendeloo GV et al (2008) Development of photocatalytic efficient titania based nanotubes and nano ribbons by conventional and microwave assisted synthesis strategies. Microporous Mesoporous Mater 114:401–409
87. Wu X, Jiang QZ, Ma ZF et al (2005) Synthesis of titania nanotubes by microwave irradiation. Solid State Commun 136:513–517
88. Arruda LB, Santos CM, Orlandi MO et al (2015) Formation and evolution of TiO_2 nanotubes in alkaline synthesis. Ceram Int 41:2884–2891
89. Hoyer P (1996) Formation of titanium oxide nanotube array. Langmuir 12:1411–1413
90. Ou HH, Lo SL (2007) Review of titania nanotube synthesized via hydrothermal treatment: fabrication, modification and application. Sep Purif Technol 58:179–191
91. Yin H, Liu H, Shen WZ (2010) The large diameter and fast growth of self-organized TiO_2 nanotube arrays achieved via electrochemical anodization. Nanotechnology 21:035601
92. Mura F, Masci A, Pasquali M et al (2009) Effect of a galvanostatic treatment on the preparation of highly ordered TiO_2 nanotubes. Electrochim Acta 54:3794–3798
93. Jang SH, Choe HC, Ko YM et al (2009) Electrochemical characteristics of nanotubes formed on Ti-Nb alloys. Thin Solid Films 517:5038–5043
94. Tsuchiya H, Akaki T, Nakata J et al (2009) Anodic oxide nanotube layers on Ti-Ta alloys: substrate composition, microstructure and self-organization on two-size scales. Corros Sci 51:1528–1533
95. Xu R, Zhao J, Tao J et al (2008) Fabrication of Ti-Al-Zr alloy oxide nanotube arrays in organic electrolytes by anodization. J Appl Electrochem 38:1229–1232
96. Yasuda K, Schmuki P (2007) Control of morphology and composition of self-organised zirconium titanate nanotubes formed in (NH4)2SO4/NH4F electrolytes. Electrochim Acta 52:4053–4061
97. Tsuchiya H, Macak JM, Ghicov A et al (2006) Nanotube oxide coating on Ti–29Nb–13Ta–4.6Zr alloy prepared by self-organizing anodization. Electrochim Acta 52:94–101
98. Mohan L, Anandan C, Rajendran N (2015) Electrochemical behavior and bioactivity of self-organized TiO_2 nanotubes on Ti-6Al-4V in Hank's solution for biomedical applications. Electrochim Acta 155:411–420
99. Mohan L, Anandan C, Rajendran N (2015) Electrochemical behavior and effect of heat treatment on morphology, crystalline structure of self-organized TiO_2 nanotube arrays on Ti-6Al-7Nb for biomedical applications. Mater Sci Eng C 50:394–401
100. Frandsen CJ, Brammer KS, Noh K et al (2014) Tantalum coating on TiO_2 nanotubes induces superior rate of matrix mineralization and osteofunctionality in human osteobalsts. Mater Sci Eng C 37:332–341
101. Ntho TA, Anderson JA, Scurrell MS (2009) CO oxidation over titanate nanotube supported Au: deactivation due to bicarbonate. J Catal 261:94–100
102. Esfahani MN, Habibi MH (2008) Silver doped TiO_2 nanostructure composite photocatalyst film synthesized by sol-gel spin and dip coating technique on glass. Int J Photoenergy 2008:1–11
103. Yu J, Dai G, Huang B (2009) Fabrication and characterization of visible-light-driven plasmonic photocatalyst Ag/AgCl/TiO_2 nanotube arrays. J Phys Chem C 113:16394–16401
104. Li H, Duan X, Liu G et al (2008) Photochemical synthesis and characterization of Ag/TiO_2 nanotube composites. J Mater Sci 43:2008
105. Khan MA, Han DH, Yang OB (2009) Enhanced photoresponse towards visible light in Ru doped titania nanotube. Appl Surf Sci 255:3687–3690
106. Lu N, Zhao H, Li J (2008) Characterisation of boron-doped TiO_2 nanotube arrays prepared by electrochemical method and its visible light activity. Sep Purif Technol 62:668–673
107. Kontos AI, Likodimos V, Stergiopoulus T et al (2009) Self-organised TiO_2 nanotube arrays functionalized by iron oxide nanoparticle. Chem Mater 21:662–672
108. Fu Y, Wei ZD, Chen SG et al (2009) Synthesis of Pd/TiO_2 nanotubes/Ti for oxygen reduction in acidic solution. J Power Sour 189:982–987
109. Yang L, Xiao Y, Zeng G et al (2009) Fabrication and characterization of Pt/C-TiO_2 nanotube arrays as anode material for methanol electrocatalytic oxidation. Energy Fuels 23:3134–3138
110. Yin Y, Tan X, Hou F et al (2009) Efficient synthesis of titania nanotube and enhanced photoresponse of Pt decorated TiO_2 for water splitting. Front Chem Eng China 3:298–304
111. Kim DH, Suk JJ, Soo HS et al (2009) High electrochemical li intercalation in titanate nanotubes. J Phys Chem C 113:14034–14039
112. Zhu W, Wang G, Hong X (2009) Metal nanoparticle chains embedded in TiO_2 nanotubes prepared by one-step electrodeposition. Electrochim Acta 55:480–484
113. Zhang S, Chen Y, Yu Y et al (2008) Synthesis, characterization of Cr-doped TiO_2 nanotubes with high photocatalytic activity. J Nanoparticle Res 10:871–875
114. Xu YH, Chen C, Yang XL et al (2009) Preparation, characterization and photocatalytic activity of the neodymium-doped TiO_2 nanotubes. Appl Surf Sci 255:8624–8628
115. Indira K, Mudali UK, Rajendran N (2014) In-vitro biocompatibility and corrosion resistance of strontium incorporated TiO_2 nanotube arrays for orthopaedic applications. J Biomater Appl 29(1):113–129
116. Zhao L, Wang H, Huo K et al (2013) The osteogenic activity of strontium loaded tittania nanotube arrays on titanium substrates. Biomater 34:19–29
117. Indira K, Kamachi Mudali U, Rajendran N (2014) In-vitro bioactivity and corrosion resistance of Zr incorporated TiO_2 nanotube arrays for orthopaedic applications. Appl Surf Sci 316:264–275
118. Liu H, Liu G, Zhou Q (2009) Preparation and characterization of Zr doped TiO_2 nanotube arrays on the titanium sheet and their enhanced photocatalytic activity. J Solid State Chem 182:3238–3242
119. Hu X, Zhang T, Jin Z (2008) Fabrication of carbon modified TiO_2 nanotube arrays and their photocatalytic activity. Mater Lett 62:4579–4581
120. Guo Y, Lee NH, Oh HJ et al (2008) Preparation of titanate nanotube thin films using hydrothermal method. Thin Solid Films 516:8363–8371
121. Park JH, Kim S, Bard AJ (2006) Novel carbon doped TiO_2 nanotube arrays with high aspect ratio for efficient solar water splitting. Nano Lett 6:24–28
122. Kilin N, Sennik E, Isik M et al (2014) Fabrication and gas sensing properties of C-doped and un-doped TiO_2 nanotubes. Ceram Int 40:109–115

123. Kim D, Fujimoto S, Schmuki P et al (2008) Nitrogen doped anodic TiO_2 nanotubes grown from nitrogen containing Ti alloys. Electrochem Commun 10:910–913
124. Shanker K, Tep KC, Mor GK et al (2006) An electrochemical strategy to incorporate nitrogen in nanostructured TiO_2 thin films: modification of band gap and photoelectrochemical properties. J Phys D Appl Phys 39:2361–2366
125. Su Y, Zhang X, Han S et al (2007) F-B-codoping of anodized TiO_2 nanotubes using chemical vapour deposition. Electrochem Commun 9:2291–2298
126. Zhu Q, Hu H, Li G (2014) TiO_2 nanotube arrays grafted with MnO_2 nanosheets as high performance anode for lithium ion batteries. Electrochim Acta 156:252–260
127. Loget G, Yoo JE, Mazare A et al (2015) Highly controlled coating of biomimetic polydopamine in TiO_2 nanotubes. Electrochem Commun 52:41–44
128. Yan X, Zhang X, Mao H et al (2015) Hydroxyapatite/gelatin functionalized graphene oxide composite coatings deposited on TiO_2 nanotube by electrochemical deposition for biomedical applications. Appl Surf Sci 329:76–82
129. Alivov Y, Klopfer M, Molloi S (2010) TiO_2 nanotubes as a cold cathode for x-ray generation. Appl Phys Lett 96:243502-1
130. Chen X, Liu W, Tang L et al (2014) Electrochemical sensor for detection of hydrazine based on Au@Pd core–shell nanoparticles supported on amino-functionalized TiO_2 nanotubes. Mater Sci Eng C 34:304–310
131. Luan X, Chen L, Zhang J et al (2013) Electrophoretic deposition of reduced graphene oxide nanosheets on TiO_2 nanotube arrays for dye-sensitized solar cells. Electrochim Acta 111:216–222
132. Taveira LV, Macak JM, Sirotna K et al (2005) Initiation and growth of self-organised TiO_2 nanotubes anodically formed in NH4F/(NH4)2SO4 electrolytes. J Electrochem Soc 152:B405–B410
133. Tsuchiya H, Macak JM, Ghicov A (2007) Characterization of electronic properties of TiO_2 nanotube films. Corros Sci 49:203–210
134. Yang Y, Wang X, Li L (2008) Synthesis and growth mechanism of graded TiO_2 nanotube arrays by two step anodization. Mater Sci Eng B 149:58–62
135. Vega V, Cerdeira MA, Prida VM et al (2008) Electrolyte influence on the anodic synthesis of TiO_2 nanotube arrays. J Non-Cryst Solids 354:5233–5235
136. Tsuchiya H, Macak JM, Taveira L et al (2005) Self-organised TiO_2 nanotube prepared in ammonium fluoride containing acetic acid electrolytes. Electrochem Commun 7:576–580
137. Gong DW, Grimes CA, Singh RS (2001) Titanium oxide nanotube arrays prepared by anodic oxidation. J Mater Res 16:3331–3334
138. Indira K, Ningshen S, Kamachi Mudali U, Rajendran N (2012) Effect of anodization parameters on the structural morphology of titanium in fluoride containing electrolytes. Mater Charact 71:58–65
139. Tsuchiya H, Macak JM, Ghicov A et al (2005) Self-organised porous TiO_2 and ZrO_2 produced by anodization. Corros Sci 47:3324–3335
140. Zhao J, Wang X, Li L (2005) Electrochemical fabrication of well-ordered titania nanotubes in H3PO4/HF electrolytes. Electron Lett 41:771–772
141. Bae C, Yoon Y, Yoo H (2009) Controlled fabrication of multiwall anatase TiO_2 nanotubular architectures. Chem Mater 21:2574–2576
142. Chen X, Schriver M, Suen T et al (2007) Fabrication of 10 nm diameter TiO_2 nanotube arrays by titanium anodization. Thin Solid Films 515:8511–8514
143. Ryu WH, Park CJ, Kwon HS (2008) Synthesis of highly ordered TiO_2 nanotube in malonic acid solution by anodization. J Nanosci Nanotechnol 18:1–4
144. Tian T, Xiao XF, Liu RF (2007) Study on titania nanotube arrays prepared by Ti anodization in NH4F/H2SO4 solution. J Mater Sci 42:5539–5543
145. Xue Y, Sun Y, Wang G et al (2015) Effect of NH4F concentration and controlled charge consumption on the photocatalytic hydrogen generation of TiO_2 nanotube arrays. Electrochim Acta 155:312–320
146. Hahn R, Macak JM, Schmuki P (2007) Rapid anodic growth of TiO_2 and WO_3 nanotubes in fluoride free electrolytes. Electrochem Commun 9:947–952
147. Richter C, Panaitescu E, Willey R et al (2007) Titania nanotubes prepared by anodization in fluoride free acids. J Mater Res 22:1624–1631
148. Raja KS, Gandhi T, Misra M (2007) Effect of water content of ethylene glycol as electrolyte for synthesis of ordered titania nanotubes. Electrochem Commun 9:1069–1076
149. Yoriya S, Kittimeteeworakul W, Punprasert N (2012) Effect of anodization parameters on morphologies of TiO_2 nanotube arrays and their surface properties. J Chem Chem Eng 6:686–691
150. Macak JM, Sirotna K, Schmuki P (2005) Self-organised porous titanium oxide prepared in $Na2SO_4$/NaF electrolytes. Electrochim Acta 50:3679–3684
151. Paulose M, Varghese OK, Mor GK et al (2006) Unprecedented ultra-high hydrogen gas sensitivity in undoped titania nanotubes. Nanotechnology 17:398–402
152. Balaur E, Macak JM, Tsuchiya H et al (2005) Wetting behavior of layers of TiO_2 nanotubes with different diameter. J Mater Chem 15:4488–4491
153. Liu YB, Zhou BX, Li JH et al (2009) Preparation of short, robust and highly ordered TiO_2 nanotubes arrays and their applications as electrode. Appl Catal B 92:326–332
154. Varghese K, Gong D, Paulose M et al (2008) Hydrogen sensing using titania nanotubes. Sens Actuators B93:338–344
155. Ghicov A, Tsuchiya H, Macak JM et al (2005) Titanium oxide nanotubes prepared in phosphate electrolytes. Electrochem Commun 7:505–509
156. Macak JM, Schmuki P (2006) Anodic growth of Self-organized anodic TiO_2 nanotubes in viscous electrolytes. Electrochem Acta 52:1258–1264
157. Sun KC, Chen YC, Kuo MY et al (2011) Synthesis and characterization of highly ordered TiO_2 nanotube arrays for hydrogen generation via water splitting. Mater Chem Phys 129:35–39
158. Macak JM, Tsuchiya H, Taveira L et al (2005) Smooth anodic TiO_2 nanotubes. Angew Chem Int Ed 44:7463–7465
159. Indira K, Ningshen S, Kamachi Mudali U, Rajendran N (2011) Effect of electrolyte temperature on the surface morphology of anodized Ti. In: Jayakumar S, Kannan MD, Balasundaraprabhu R, Prassana S (eds) Thin film and nanomaterials, advanced research series. Macmillan, India, pp 63–66
160. Chen J, Lin J, Chen X (2010) Self-assembled TiO_2 nanotube arrays with U-shaped profile by controlling anodization temperature. J Nanomater. doi:10.1155/2010/753253
161. Wang J, Lin Z (2009) Anodic formation of ordered TiO_2 nanotube arrays: effects of electrolyte temperature and anodization potential. J Phys Chem C 113:4026–4030
162. Joo S, Muto I, Hara N (2008) In situ ellipsometric analysis of growth processes of anodic TiO_2 nanotube films. J Electrochem Soc 155:C154–C161
163. Li Y, Ma Q, Han J et al (2014) Controlled preparation, growth mechanism and properties research of TiO_2 nanotube arrays. Appl Surf Sci 297:103–108

164. Regonini D, Clemens FJ (2015) Anodized TiO_2 nanotubes: effect of anodizing time on film length, morphology and photo electrochemical properties. Mater Lett 142:97–101
165. Xin W, Meng C, Jie W et al (2010) Morphology dependence of TiO_2 nanotube arrays on anodization variables and buffer medium. J Semicond 31:063003-1–063003-5
166. So S, Lee K, Schmuki P (2012) Ultrafast growth of highly ordered anodic TiO_2 nanotubes in Lactic acid electrolyte. J Am Chem Soc 134:11316–11318
167. Sreekantan S, Saharudin KA, Wei LC (2011) Formation of TiO_2 nanotubes via anodization and potential applications for photocatalysts, biomedical materials, and photoelectrochemical cell. IOP Conf Series: Mater Sci Eng 21:012002. doi:10.1088/1757-899X/21/1/012002
168. Allam NK, Grimes CA (2008) Effect of cathode material on the morphology and photoelectrochemical properties of vertically oriented TiO_2 nanotube arrays. Solar Energy Mater Solar Cells 92:1468–1475
169. Yoriya S (2012) Effect of inter-electrode spacing on electrolyte properties and morphologies of anodic TiO_2 nanotube array films. Int J Electrochem Sci 7:9463
170. Setzu S, Ferrand P, Lerondel G (2002) Photo-lithography for 2D optical microstructure in porous silica: application to nucleation of macropores. Appl Surf Sci 186:588–593
171. Thompson GE (1997) Porous anodic alumina: fabrication, characterisation and applications. Thin Solid Films 297:192–201
172. Raja KS, Misra M, Paramaguru K (2005) Formation of self-ordered nano-tubular structure of anodic oxide layer on titanium. Electrochim Acta 51:154–165
173. Kim D, Stein FS, Hahn R (2008) Gravity assisted growth of self-organised anodic oxide nanotube on Ti. Electrochem Commun 10:1082–1086
174. Yin Y, Jin Z, Hou F et al (2007) Synthesis and morphology of TiO_2 nanotube arrays by anodic oxidation using modified glycerol-based electrolytes. J Am Ceram Soc 90:2384–2389
175. Lee G, Choi JW, Lee SE et al (2009) Formation behavior of TiO_2 nanotube in fluoride containing electrolytes. Trans Nonferrous Metals Soc China 19:842–845
176. Kar A, Raja KS, Misra M (2006) Electrodeposition of hydroxyapatite onto nanotubular TiO_2 for implant applications. Surf Coat Technol 201:3723–3731
177. Bai J, Zhou B, Li L et al (2008) The Formation mechanism of titania nanotube arrays in hydrofluoric acid electrolyte. J Mater Sci 43:1880–1884
178. Macak JM, Tsuchiya H, Schmuki P (2005) High-aspect-ratio TiO_2 nanotubes by anodization of titanium. Angew Chem Int Ed 44:2100–2102
179. Macak JM, Hildebrand H, Marten-Jahns U et al (2008) Mechanistic aspects and growth of large diameter self-organized TiO_2 nanotubes. J Electroanal Chem 621:254–266
180. Anitha VC, Menon D, Nair SV et al (2010) Electrochemical tuning of titania nanotube morphology in inhibitor electrolytes. Electrochim Acta 55:3703–3713
181. Mor GK, Varghese OK, Paulose M et al (2003) A self-cleaning, room-temperature titania-nanotube hydrogen gas sensor. Sensor Lett 1:42–46
182. Shankar K, Paulose M, Mor GK (2005) A study on the spectral photoresponse and photoelectrochemical properties of flame-annealed titania nanotube-arrays. J Phys D Appl Phys 38:3543–3549
183. Paramasivam I, Macak JM, Selvam T (2008) Electrochemical synthesis of self-organised TiO_2 nanotubular structures using an ionic liquid (B MIM-BF4). Electrochim Acta 54:643–648
184. Kanta AF, Poelman M, Decroly A (2015) Electrochemical characterization of TiO_2 nanotube array photo anodes for dye sensitized solar cell applications. Solar Energy Mater Solar Cells 133:76–81
185. Kim SY, Kim YK, Park IS (2014) Effect of alkali and heat treatments for bioactivity of TiO_2 nanotubes. Appl Surf Sci 321:412–419
186. Liu SM, Gan LM, Liu L et al (2002) Synthesis of single-crystalline TiO_2 nanotubes. Chem Mater 14:1391–1397
187. Yu J, Wang B (2010) Effect of calcination temperature on morphology and photoelectrochemical properties of anodized titanium dioxide nanotube arrays. Appl Catal B 94:295–302
188. Wang J, Lin Z (2009) Anodic formation of ordered TiO_2 nanotubes arrays: effect of electrolyte temperature and anodization potential. J Phys Chem C 113:4026–4030
189. Xiao X, Ouyang K, Liu R et al (2009) Anatase type titania nanotube arrays direct fabricated by anodization without annealing. Appl Surf Sci 255:3659–3663
190. Fahim NF, Sekino T (2009) A novel method for synthesis of titania nanotube powders using rapid breakdown anodization. Chem Mater 21:1967–1979
191. Zhao J, Wang X, Sun T et al (2007) Crystal phased transition and properties of Titanium oxide nanotube arrays prepared by anodization. J Alloys Compd 434–435:792–795
192. Jaroenworaluck A, Regonini D, Bowen CR et al (2010) A microscopy study of the effect of heat treatment on the structure and properties of anodized TiO_2 nanotubes. Appl Surf Sci 256:2672–2679
193. Tighineanu T, Albu RS, Hahn R et al (2010) Conductivity of TiO_2 nanotubes: influence of annealing time and temperature. Chem Phys Lett 494:260–263
194. Arunchandran C, Ramya S, George RP et al (2013) Corrosion inhibitor storage and release property of TiO_2 nanotube powder synthesized by rapid breakdown anodization method. Mater Res Bull 48:635–639
195. Cao C, Zhang G, Song X et al (2011) Morphology and microstructure of as-synthesized anodic TiO_2 nanotube arrays. Nanoscale Res Lett 6:64
196. Lim YC, Zainal Z, Hussein MZ et al (2013) The effect of heat treatment on phase transformation, morphology and photoelectrochemical response of short TiO_2 nanotubes. Digest J Nanomater Biostr 8:167–176
197. Zhao J, Wang X, Sun T et al (2007) Crystal phase transition and properties of titanium nanotube arrays prepared by anodization. J Alloy Compd 434–435:792–795
198. Xiao P, Liu D, Garcia BB et al (2008) Electrochemical and photoelectrical properties of titania nanotube arrays annealed in different gases. Sensor Actuat B: Chem 134:367–372
199. Beranek R, Hildebrand H, Schmuki P (2003) Self-organized porous titanium oxide prepared in H2SO4/HF electrolytes. Electrochem Solid-State Lett 6:B12
200. Bestetti M, Franz S, Cuzzolin M et al (2007) Structure of nanotubular titanium oxide templates prepared by electrochemical anodization in H2SO4/HF solutions. Thin Solid Films 515:5253–5258
201. Zeng X, Gan YX, Clark E (2011) Amphiphilic and photocatalytic behaviors of TiO_2 nanotube arrays on Ti prepared via electrochemical oxidation. J Alloy Compd 509:L221–L227
202. Brammer KS, Oh S, Cobb CJ et al (2009) Improved bone-forming functionality on diameter-controlled TiO_2 nanotube surface. Acta Biomater 5:3215–3223
203. Narayanan R, Kwon TY, Kim KH (2009) TiO_2 nanotubes from stirred glycerol/NH4F electrolyte: roughness, wetting behavior and adhesion for implant applications. Mater Chem Phys 117:460–464
204. Wang F, Shi L, He WX et al (2013) Bioinspired micro/nano fabrication on dental implant–bone interface. Appl Surf Sci 265:480–488
205. Munirathinam B, Neelakantan L (2015) Titania nanotubes from weak organic acid electrolyte: fabrication, characterization and oxide film properties. Mater Sci Eng C 49:567–578

206. Liu Q, Wu X, Wang B et al (2002) Preparation and superhydrophilic properties of TiO_2/SiO_2 composite thin films. Mater Res Bull 37:2255–2262
207. Brammer KS, Oh S, Frandsen CJ et al (2011) Biomaterials and biotechnology schemes utilizing TiO_2 nanotube arrays in Biomater Sci Eng Rosario Pignatello (Eds) ISBN 978-953-307-609-6
208. Lu K, Tian Z, Geldmeier JA (2011) Polishing effect on anodic titania nanotube formation. Electrochim Acta 56:6014–6020
209. Sun L, Zhang S, Sun X et al (2010) Effect of the geometry of titania nanotube array on the performance of dye sensitized solar cells. J Nanosci Nanotechnol 10:4551–4561
210. Shankar K, Mor GK, Prakasam HE et al (2007) Highly ordered TiO_2 nanotube arrays up to 220 m in length: use in water photoelectrolysis and dye sensitized solar cells. Nanotechnology 18:065707. doi:10.1088/0957-4484/18/6/065707
211. Shankar K, Basham KI, Allam NK et al (2009) Recent advantages in the use of TiO nanotube and nanowire arrays for oxidative photoelectrochemistry. J Phys Chem C 113:6327–6359
212. Oh S, Daraio C, Chen LH et al (2006) Significantly accelerated osteoblast cell growth on aligned TiO_2 nanotubes. J Biomed Meters Res Part A 78:97–103
213. Tran N, Webster TJ (2009) Nanotechnology for bone materials, 1st edn. Wiley, New York, pp 336–351
214. Ercan B, Webster TJ (2008) Greater osteoblast proliferation on anodized nanotubular Ti upon electrical stimulation. Int J Nanomed 3:817–821
215. Xiao XF, Liu RF, Tian T (2008) Preparation of bioactive titania nanotube arrays in HF/Na2HPO4 electrolyte. J Alloys Compd 466:356–362
216. Zhao L, Mei S, Chu PK et al (2010) The influence of hierarchical hybrid micro/nano-textured titanium surface with titania nanotubes on osteoblast functions. Biomater 31:5072–5082
217. Bauer S, Park J, Mark KVD et al (2008) Improved attachment of mesenchymal stem cells on super-hydrophobic TiO_2 nanotubes. Acta Biomater 4:1576–1582
218. Navarro M, Michiardi A, Castano O et al (2008) Biomaterials in orthopaedics. J R Soc Interface 5:1137–1158
219. Crawford GA, Chawla N, Das K et al (2007) Microstructure and deformation behavior of biocompatible TiO_2 nanotubes on titanium substrate. Acta Biomater 3:359–367
220. Oh S, Jin S (2006) Titanium oxide nanotubes with controlled morphology for enhanced bone growth. Mater Sci Eng C 26:1301–1306
221. Webster TJ, Seigel RW, Bizios R (2000) Enhanced functions of osteoblasts on nanophase ceramics. Biomater 21:1803–1810
222. Mor GK, Varghese OK, Paulose M et al (2006) A Review on highly ordered, vertically oriented TiO_2 nanotube arrays: fabrication, material properties, and solar energy applications. Solar Energy Mater Solar Cells 90:2011–2075
223. Kodama A, Bauer S, Komatsu A et al (2009) Bioactivation of titanium surfaces using coatings of TiO_2 nanotubes rapidly pre-loaded with synthetic hydroxyapatite. Acta Biomater 5:2322–2330
224. Indira K, Kamachi Mudali U, Rajendran N (2013) Corrosion behavior of electrochemically assembled nanoporous titania for biomedical applications. Ceram Int 39:959–967
225. Indira K (2015) Development of titanium nanotube arrays for orthopaedic applications. Dissertation, Anna University, http://shodhganga.inflibnet.ac.in/handle/10603/37614
226. Parcharoen Y, Kajitvichyanukul P, Sirivisoot S et al (2014) Hydroxyapatite electrodeposition on anodized titanium nanotubes for orthopedic applications. Appl Surf Sci 311:54–61
227. Huang Q, Yung Y, Hu R et al (2015) Reduced platelet adhesion and improved corrosion resistance of superhydrobhophic TiO_2 nanotube coated 316L stainless steel. Colloids Surf B: Biointerface 125:34–141
228. Mohan L, Anandan C, Rajendran N (2015) Effect of plasma nitriding on structure and biocompatibility of self-organized TiO_2 nanotubes on Ti-6Al-7Nb. RSC Adv 5:41763–41771
229. Popat KC, Leoni L, Grimes CA et al (2007) Influence of engineered titania nanotubular surfaces on bone cells. Biomater 28:3188–3197
230. Park J, Bauer S, Mark KVD et al (2007) Nanosize and vitality: TiO_2 nanotube diameter directs cell fate. Nano Lett 7:1686–1691
231. Antonio JAT, Cortes-Jacome MA, Angeles-Chavez C et al (2009) Highly quasi-monodisperse Ag nanoparticles on titania nanotubes by impregnative aqueous ion exchange. Langmuir 25:10195–10201
232. Ainslie KM, Tao SL, Popat KC et al (2009) In vitro inflammatory response of nanostructured titania, silicon oxide, and polycaprolactone. J Biomed Mater Res A 91:647–655
233. Brammer KS, Oh S, Gallagher JO, Jin S (2008) Enhanced cellular mobility studies guided by TiO_2 nanotube surfaces. Nano Lett 8:786–793
234. Peng L, Eltgroth ML, Tempa TJL et al (2009) The effect of TiO_2 nanotubes on endothelial function and smooth muscle proliferation. Biomater 30:1268–1272
235. Lan MY, Lee SL, Huang HH et al (2014) Diameter selective behavior of human nasal epithelial cell on Ag-coated TiO_2 nanotubes. Ceram Int 40:4745–4751
236. Wang Y, Wang J, Deng X et al (2009) Direct imaging of titania nanotubes located in mouse neural stem cell nuclei. Nano Res 2:543–552
237. Kasuga T, Hiramatsu M, Hoson A et al (1998) Formation of titanium oxide nanotube. Langmuir 14:3160–3163
238. Kalbacova M, Macak JM, Stein FS et al (2008) TiO_2 nanotubes: photocatalyst for cancer cell killing. Phys Stat Sol 2:194–196
239. Chen X, Cai K, Fang J et al (2013) Fabrication of selenium-deposited and chitosan-coated titania nanotubes with anticancer and antibacterial properties. Colloids Surf B: Biointerface 103:149–157
240. Ng ClarisseCH, Liao S, Chan CK (2009) Drug delivery and titanium dioxide nanotubes. Nanomedicine 4:381–383
241. Xilin X, Yang L, Guo M et al (2009) Biocompatibility and in vitro anti-neoplastic drug-loaded trial of titania nanotubes prepared by anodic oxidation of a pure titanium. Sci China Ser B: Chem 52:2161–2165
242. Signoretto M, Ghedini E, Nichele V et al (2011) Effect of textural properties on the drug delivery behaviour of nanoporous TiO_2 matrices. Microporous Mesoporous Mater 139:189–196
243. Moseke C, Hage F, Vorndran E et al (2012) TiO_2 nanotube arrays deposited on Ti substrate by anodic oxidation and their potential as a long-term drug delivery system for antimicrobial agents. Appl Surf Sci 258:5399–5404
244. Mandal SS, Jose D, Bhattacharyya AJ (2014) Role of surface chemistry in modulating drug release kinetics in titania nanotubes. Mater Chem Phys 147:247–253
245. Chennell P, Feschet-Chassot E, Deversc T et al (2013) In vitro evaluation of TiO_2 nanotubes as cefuroxime carriers on orthopaedic implants for the prevention of periprosthetic joint Infections. Int J Pharm 455:298–305
246. Hu Y, Cai K, Luo Z et al (2012) TiO_2 nanotubes as drug nanoreservoirs for the regulation of mobility and differentiation of mesenchymal stem cells. Acta Biomater 8:439–448
247. Wang Z, Xie C, Luo F et al (2015) P25 nanoparticles decorated TiO_2 nanotube arrays as effective drug delivery system for ibuprofen. Appl Surf Sci 324:621–626
248. Gulati K, Ramakrishnan S, Aw MS et al (2012) Biocompatible polymer coating of titania nanotube arrays for improved drug elution and osteoblast adhesion. Acta Biomater 8:449–456